

AD-A038 645

ARMY ARMAMENT MATERIEL READINESS COMMAND ROCK ISLAND --ETC F/G 17/7
SYSTEMS ANALYSIS DIRECTORATE ACTIVITIES SUMMARY JANUARY 1977. (U)
FEB 77

UNCLASSIFIED

DRSAR/SA/N-63

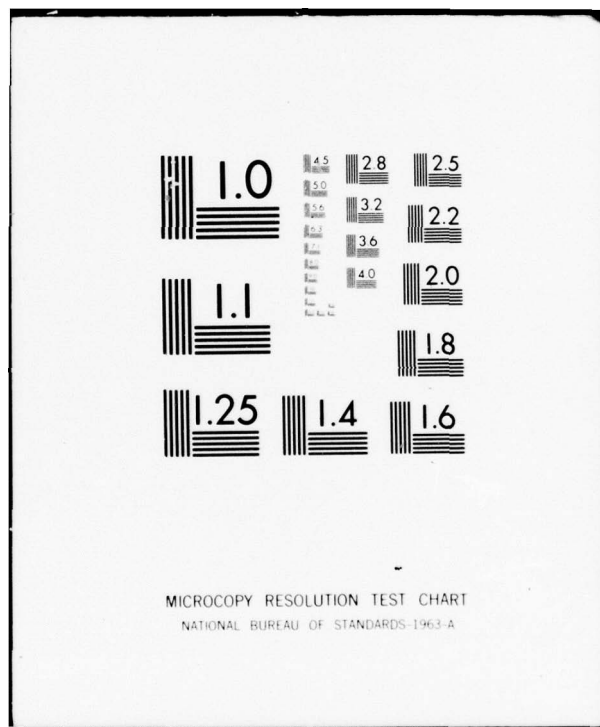
NL

| OF |
AD
A038645



END

DATE
FILMED
5-77



ADA 038645

1
12
NW

AD

DRSAR/SA/N-63

SYSTEMS ANALYSIS DIRECTORATE
ACTIVITIES SUMMARY
JANUARY 1977

FEBRUARY 1977

Approved for public release; distribution unlimited.



US ARMY ARMAMENT MATERIEL READINESS COMMAND
SYSTEMS ANALYSIS DIRECTORATE
ROCK ISLAND, ILLINOIS 61201

No. _____
FILE COPY

DISPOSITION

Destroy this report when no longer needed. Do not return it to the originator.

DISCLAIMER

The findings in this report are not to be construed as an official Department of the Army position.

WARNING

Information and data contained in this document are based on input available at the time of preparation. Because the results may be subject to change, this document should not be construed to represent the official position of the US Army Development & Readiness Command unless so stated.

UNCLASSIFIED

SECURITY CLASSIFICATION OF THIS PAGE (When Data Entered)

DD FORM 1 JAN 72 1473

EDITION OF 1 NOV 65 IS OBSOLETE

UNCLASSIFIED

SECURITY CLASSIFICATION OF THIS PAGE (When Data Entered)

CONTENTS

| | <u>Page</u> |
|---|-------------|
| Section I. GENERAL | 5 |
| Section II. MEMORANDA AND OTHER TECHNICAL INFORMATION | 7 |
| Description of the Process of Laser Spot Motion During Designation of Moving Targets | 11 |
| Cost Differential (COSDIF) Probabilities | 65 |
| DISTRIBUTION LIST | 75 |

ASSIGNMENT

| | | |
|---------------------------------|-----------------------|-------------------------------------|
| 210 | White Section | <input checked="" type="checkbox"/> |
| 500 | Buff Section | <input type="checkbox"/> |
| UNANNOUNCED | | |
| JUSTIFICATION | | |
| BY | | |
| DISTRIBUTION/AVAILABILITY CODES | | |
| BEST | AVAIL. END OF SP. DAY | |
| A | | |

Next page is blank.

Section I. GENERAL

1. This monthly publication summarizes the activities of the Systems Analysis Directorate. The purpose of this note is to give wider and more timely distribution on subjects of concern to the command.
2. The most significant Memoranda for Record (MFR's) and other technical information will be published as notes or reports at a later date.
3. In order to assure accurate distribution of this publication, addition or deletion of addresses to/from the DISTRIBUTION LIST are invited and should be forwarded to the address below.
4. Inquiries applicable to specific items of interest may be forwarded to Commander, US Army Armament Materiel Readiness Command, ATTN: DRSAR-SA, Rock Island, IL 61201 (AUTOVON 793-4483/4628).

Next page is blank.

Section II. MEMORANDA AND OTHER TECHNICAL INFORMATION

Memoranda for Record and other technical information are grouped according to subject, where applicable, and in chronological order.

Next page is blank.

**DESCRIPTION OF THE PROCESS OF
LASER SPOT MOTION DURING DESIGNATION
OF MOVING TARGETS**

Next page is blank.



DEPARTMENT OF THE ARMY
HEADQUARTERS, UNITED STATES ARMY ARMAMENT COMMAND
ROCK ISLAND, ILLINOIS 61201

REPLY TO
ATTENTION OF:

DRSAR-SA

21 JAN 1977

SUBJECT: Description of the Process of Laser Spot Motion During
Designation of Moving Targets

Commander
Picatinny Arsenal
ATTN: DRCPM-CAWS (Messrs. E. Manley & E. Zimpo)
Dover, NJ 07801

1. References:

- a. MFR, AMSAR-SAM, 16 Jan 76, subject: Laser Guidance Measurements Program.
 - b. MFR, DRSAR-SAM, 20 Jan 77, subject as above.
2. It is recognized that there is widespread interest in the principal sources of error in the guidance accuracy of Copperhead and HELLFIRE. Further, it has been established that laser spot motion (jitter or dither) is often the primary external error source. Over the past year attention has been given to measuring the pheonomenological components of spot motion (Ref a.).
3. With a recognition of the importance of this subject, DRSAR-SAM has prepared a memorandum which examines the spot motion phenomenon in greater detail. This attached memorandum (Ref b.) is submitted herewith for your information. The MFR should be of interest to systems analysts and to test personnel involved in the laser measurements program.
4. Briefly, the MFR treats a statistical technique for estimating the dynamic components of spot motion, makes comparisons between an analytic (theoretical) model and experiment in both the frequency- and time-domains,

DRSAR-SA

SUBJECT: Description of the Process of Laser Spot Motion During
Designation of Moving Targets

and, finally, derives the equations used in a digital computer
simulation of spot motion.

FOR THE COMMANDER:

SIGNED

1 Incl

as

M. RHIAN
Acting Director
Systems Analysis Directorate

CF:

PTA, DRCPM-CAWS (Messrs. B. Barrett & J. Williams)

AVSCOM, DRASV-WR (Mr. D. Dunlap)

MICOM, DRSMI-RGT (Mr. Lewis)

MICOM, DRSMI-RGN (Mr. Pastrick)

RSA, DRCPM-CAWS-FO (COL Nulk)

WSMR, STEWS-TE-PC (Steve Kadner)

AMSAA, DRXSY-AAM (Pat Hill)

AMSAA, DRXSY-GS (Dave Barnhardt)

DRSAR-SAM (Mr. Schlenker)

DRSAR-SACF

DRSAR-SA RF

~~DRSAR-SAM~~

DRSAR-SAM RF

SARRI-RLR (Dr. Amoruso)

DRXHE-RI (Mark Brauer & Dick Carter)

DRSAR-SAM

20 Jan 1977

MEMORANDUM FOR RECORD

SUBJECT: Description of the Process of Laser Spot Motion During Designation of Moving Targets

1. A set of references related to the above subject is found at Attachment 1.
2. Background.

In connection with the support given the Copperhead program, the undersigned has repeatedly emphasized the importance of laser spot motion as a primary error source in guided projectile performance. References [1] and [2] illustrate this emphasis. As a consequence of the importance attached to spot motion and other aspects of the laser signature, considerable efforts have been spent studying tracking error for various designators and trackers. Some analytic models of the tracking error are given in References [3] and [4]. In particular, Reference [4] describes the statistical techniques used to produce an analytic model descriptive of the tracking error of the Ground Laser Locator Designator (GLLD) observed during the CLGP OT-1 Tracking Tests. All of these models are suitable for a digital simulation of the stochastic process of spot motion, which can be used as input to terminal guidance simulations.

3. An accurate characterization of laser spot motion, whatever its source, is also important because (stochastic) process dynamics are also pertinent to the problem of laser spillover and its consequence for guidance accuracy. In Reference [5], which addresses this problem, spot motion dynamics were, simply, assumed.

4. In an effort to standardize laser designator testing procedures, increased attention (Reference [6]) has been given to various phenomena which give rise to laser spot motion: device jitter, atmospheric propagation effects (scintillation), and designator tracking error. In a field-test environment, these phenomena all contribute and cannot be isolated by direct measurement. Consequently, some of the past analyses, which have considered "spot motion" and "tracking error" as interchangeable terms, have been somewhat indiscriminate. Pragmatically this lack of attention to the components of spot motion may not have been of great significance in that the joint process is what is of concern in guided projectile accuracy analysis. However, a closer attention to the components of spot motion does produce clarity in understanding the disparate phenomena.

5. Outline of Memorandum.

This memorandum reexamines some of the spot motion data from the CLGP

DRSAR-SAM

SUBJECT: Description of the Process of Laser Spot Motion During Designation of Moving Targets

OT-1 Tracking Tests with the intention of isolating by statistical means the component attributable to the human tracking error from those produced by other mechanisms. For notational simplicity, throughout the balance of this paper, device jitter and beam-steering effects due to the atmosphere will be subsumed by the term "scintillation component." This oversimplification is considered justifiable because of the dominance of atmospheric effects in the examples treated. In decomposing laser spot motion into tracking and scintillation components, we exploit the fact that these components have different dynamics which are nearly separable in the frequency domain.

6. Because the analysis, comparison with experimental data, and algorithmic description of spot motion components is lengthy, these mathematical developments are divided into five separate and nearly independent annexes:

- Annex 1. Decomposition of Laser Spot Motion into Tracking and Scintillation Components.
- Annex 2. The Analytical Covariance Function for Laser Spot Motion Developed From the Spectral Density.
- Annex 3. Digital Computer Implementation for the First-Order Component of the Spot Motion Error.
- Annex 4. Digital Computer Implementation for the Second-Order Component of the Spot Motion Error.
- Annex 5. Autospectra of the Digital Error Processes.

7. Summary.

In Annex 1 it is argued that the autospectrum of spot motion consists mainly of separable, additive components: one due to the human tracking process, possessing approximately second-order dynamics, and the other due to processes having approximately first-order dynamics with a significantly higher crossover frequency than the human tracker component. Expressions for the gain constant in each component of the autospectrum are developed in terms of the variance of each component. A numerical example of the analytic autospectrum is compared with an experimental estimate derived from the azimuthal error of Run 75A of the CLGP OT-1 Tracking Tests. Parameter values of the analytic model were selected by trial and error, under constraints, to produce an acceptable Chebychev fit to the experimental autospectrum in the sense of minimizing the maximum residual.

8. It is sometimes useful to make comparisons between analytic models and experimental estimates in the time domain as well as in the frequency domain.

DRSAR-SAM

SUBJECT: Description of the Process of Laser Spot Motion During Designation of Moving Targets

One place where such a comparison is useful is in guided flight simulations in which a long experimental record of spot motion is employed directly as input. With the autocorrelation (or autocovariance) function one can maximize the number of statistically independent replications obtainable from the record. Annex 2 develops an expression for the autocovariance function for the (joint) spot motion process and extends the example of Annex 1 by comparing the autocorrelation function of the analytic model with an experimental estimate.

9. Annex 3 treats the digital implementation of the first-order component of spot motion. Implementation is achieved by low-pass filtering of gaussian white noise. Expressions are developed for the coefficients of the digital filter and for the variance of the input noise required to produce a given output process variance.

10. Annex 4 parallels the developments of Annex 3 while treating the second-order component of the spot motion process. This development is the basis of the principal algorithm* which DRSAR-SA and others have used to describe spot motion during the past four years.

11. Annex 5 develops the autospectra of the scintillation (first-order) and tracking (second-order) dynamic components as implemented digitally. The autospectrum of each component is separately compared with its continuous-time (analog) counterpart. Some sources of distortion in the digital implementation and in the process of making statistical estimates of autospectra are identified, and are quantified using the first-order process as an example.

George J. Schlenker

GEORGE J. SCHLENKER
Operations Research Analyst
Methodology Division
Systems Analysis Directorate

*A special case is presented in subroutine DITH of Reference [3].

ANNEX 1

DECOMPOSITION OF LASER SPOT MOTION INTO TRACKING AND SCINTILLATION COMPONENTS

Let the variance of the spot motion at the target due to only tracker error be σ_t^2 in (m^2). Experience with the TOW and GLLD trackers as well as airborne man-operated trackers shows that tracking error exhibits approximately second-order dynamics.

Let the tracking process be second-order Butterworth so that the spectral density is given by

$$H_t^2(v) = \frac{A}{1 + (v/v_t)^4}, \quad 0 \leq v < \infty, \quad (1.1)$$

with gain constant A and natural corner frequency v_t .

The variance or total power of the process is

$$\sigma_t^2 = \int_0^\infty H_t^2(v) dv \quad (1.2)$$

$$= A v_t \int_0^\infty \frac{df}{1 + f^4} \quad (1.3)$$

$$\sigma_t^2 = A v_t \pi \sqrt{2} / 4. \quad (1.4)$$

Whence

$$A = \frac{4 \sigma_t^2}{\sqrt{2} \pi v_t} \quad (1.5)$$

$$A = \frac{2 \sqrt{2} \sigma_t^2}{\pi v_t}. \quad (\text{m}^2/\text{hz})$$

(1-1)

Normally, the corner frequency v_t is determined by the dynamics of the human motor system and lies below one hertz.

Scintillation data suggest that the majority of scintillation power lies above one hertz at frequencies to which the human cannot respond. Consequently, tracking error noise and scintillation noise are substantially uncorrelated. Data on intensity of scintillation above 10 hertz suggest this process has nearly first-order dynamics.

We suppose that a first-order process, uncorrelated with the tracking process, with variance σ_s^2 is superposed thereon. The spectrum for this scintillation process is given by

$$H_s^2(v) = \frac{B}{1 + (v/v_s)^2}, \quad (1.6)$$

with corner frequency v_s .

Therefore,

$$\sigma_s^2 = \int_0^\infty H_s^2(v) dv \quad (1.7)$$

$$\sigma_s^2 = B v_s \int_0^\infty \frac{df}{1 + f^2} \quad (1.8)$$

$$\sigma_s^2 = B v_s \frac{\pi}{2}. \quad (1.9)$$

Whence,

$$B = \frac{2}{\pi} \frac{\sigma_s^2}{v_s} \quad (m^2/hz). \quad (1.10)$$

(1-2)

If the processes are superposed, the spectrum of the joint process is just the sum of the component spectra. Letting the joint autospectrum be $H^2(v)$, *

$$H^2(v) = H_t^2(v) + H_s^2(v) \quad (1.11)$$

$$H^2(v) = \frac{A}{1 + (v/v_t)^4} + \frac{B}{1 + (v/v_s)^2} . \quad (1.12)$$

Example

Based on daytime tracking tests at WSMR during the CLGP OT 1 Tests, the following parameter values were selected from Run 75A for the azimuthal error:

$$v_t = 0.7 \text{ hz} , \quad v_s = 3 \text{ hz}^-$$

$$\sigma_t = 0.230 \text{ m} , \quad \sigma_s = 0.165 \text{ m} \quad (\text{at } 3 \text{ km range})$$

$$A = 6.8038 \cdot 10^{-2} , \quad B = 5.7773 \cdot 10^{-3} \quad (\text{m}^2/\text{hz}).$$

Numerical results are shown in Table 1 and in Figure 1.

TABLE 1. ANALYTIC ESTIMATES OF THE TRACKING AND SCINTILLATION COMPONENTS OF AZIMUTHAL LASER SPOT MOTION IN THE AUTOSPECTRUM

| v | $H_t^2(v)$ | $H_s^2(v)$ | $H^2(v)$ | (m^2/hz) |
|-----|-----------------------|-----------------------|-----------------------|----------------------------|
| 0.3 | $6.582 \cdot 10^{-2}$ | $5.720 \cdot 10^{-3}$ | $7.154 \cdot 10^{-2}$ | |
| 0.5 | $5.398 \cdot 10^{-2}$ | $5.621 \cdot 10^{-3}$ | $5.961 \cdot 10^{-2}$ | |
| 0.7 | $3.402 \cdot 10^{-2}$ | $5.479 \cdot 10^{-3}$ | $3.950 \cdot 10^{-2}$ | |
| 1.0 | $1.317 \cdot 10^{-2}$ | $5.200 \cdot 10^{-3}$ | $1.837 \cdot 10^{-2}$ | |
| 1.5 | $3.081 \cdot 10^{-3}$ | $4.622 \cdot 10^{-3}$ | $7.702 \cdot 10^{-3}$ | |
| 2.0 | $1.006 \cdot 10^{-3}$ | $4.000 \cdot 10^{-3}$ | $5.005 \cdot 10^{-3}$ | |
| 4.0 | $6.375 \cdot 10^{-5}$ | $2.080 \cdot 10^{-3}$ | $2.144 \cdot 10^{-3}$ | |

* An alternative notation for the spectral density (autospectrum) is $\Gamma_{xx}(v)$, for azimuth, and $\Gamma_{yy}(v)$, for elevation
(1-3)

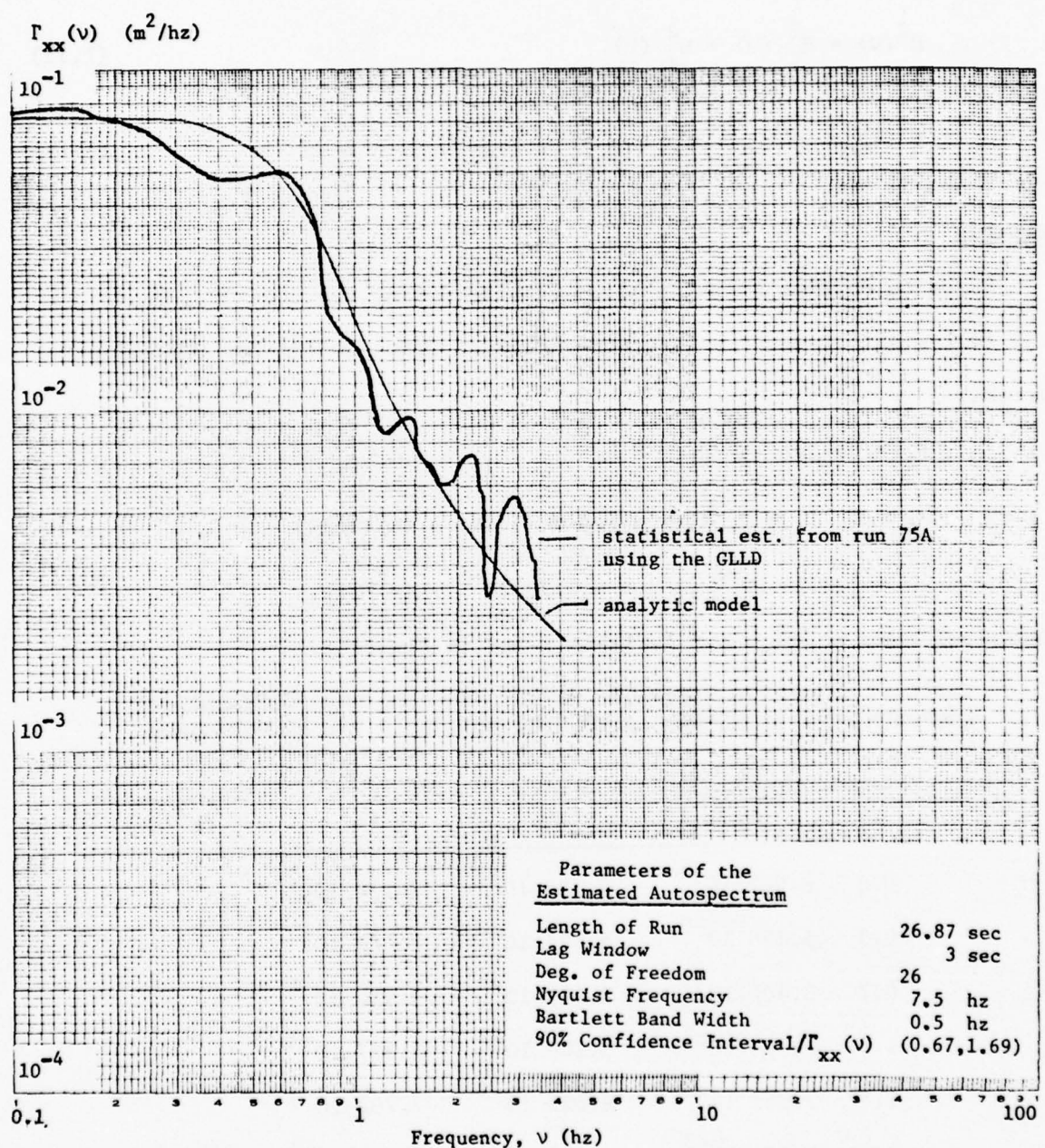


Figure 1. Comparison of an Analytic Model of the Autospectrum of Azimuthal Laser Spot Motion With an Experimental Estimate

(1-4)

ANNEX 2

THE ANALYTICAL COVARIANCE FUNCTION FOR LASER SPOT MOTION DEVELOPED FROM THE SPECTRAL DENSITY

The spectral density (autospectrum) of laser spot motion in, say, the x-direction due to the joint effects of tracking jitter and atmospheric scintillation (beam steering) is given by

$$\Gamma_{xx}(v) = \frac{A}{1+(v/v_t)^4} + \frac{B}{1+(v/v_s)^2}, \quad (2.1)$$

where

$$A = \frac{2\sqrt{2}}{\pi v_t} \sigma_t^2$$

$$B = \frac{2}{\pi v_s} \sigma_s^2,$$

with variance contributed by tracking σ_t^2 and variance contributed by scintillation σ_s^2 . By definition,

$$\sigma_t^2 + \sigma_s^2 = \int_0^\infty \Gamma_{xx}(v) dv. \quad (2.2)$$

The natural corner frequency of the second-order tracking process is v_t and that of the first-order scintillation process is v_s .

An alternative expression for (2.1) in terms of the angular frequency ω is $\Gamma'_{xx}(\omega)$.

$$\Gamma'_{xx}(\omega) = \Gamma_{xx}(v(\omega)) \left| \frac{dv}{d\omega} \right|$$

or

(2-1)

$$\Gamma'_{xx}(\omega) = \frac{1}{2\pi} \Gamma_{xx} \left(\frac{\omega}{2\pi} \right) \quad (2.3)$$

$$\Gamma'_{xx}(\omega) = \frac{A \omega_t^4 (2\pi)^{-1}}{\omega_t^4 + \omega^4} + \frac{B \omega_s^2 (2\pi)^{-1}}{\omega_s^2 + \omega^2} \quad . \quad (2.4)$$

Now, the spectral density is by definition the Fourier cosine transform of the autocovariance function $\gamma_{xx}(t)$.

$$\Gamma'_{xx}(\omega) = \frac{2}{\pi} \int_0^\infty \gamma_{xx}(t) \cos \omega t dt . \quad (2.5)$$

In general, the Fourier transform pairs $f(t)$ and $g(\omega)$ are related by:

$$g(\omega) = \int_0^\infty f(t) \cos (\omega t) dt$$

$$f(t) = 2\pi \int_0^\infty g(\omega) \cos (\omega t) d\omega . \quad (2.6)$$

From (2.5),

$$\gamma_{xx}(t) = \pi^2 \int_0^\infty \Gamma'_{xx}(\omega) \cos (\omega t) d\omega . \quad (2.7)$$

The following general results will be used to develop an expression for $\gamma_{xx}(t)$ for the spot motion process:

$$\int_0^\infty (a_1^2 + \omega^2)^{-1} \cos \omega t d\omega = (2\pi a_1)^{-1} e^{-a_1 t} \quad (2.8)$$

$$\int_0^\infty (a_2^4 + \omega^4)^{-1} \cos \omega t d\omega =$$

$$(2\pi)^{-1} a_2^{-3} e^{-a_2 t / \sqrt{2}} \sin \left(\frac{\pi}{4} + \frac{a_2 t}{\sqrt{2}} \right) . \quad (2.9)$$

(2-2)

Using the expression for $\Gamma'_{xx}(\omega)$ in (2.4),

$$\int_0^\infty \Gamma'_{xx}(\omega) \cos \omega t d\omega = B v_s (2\pi)^{-1} e^{-\omega_s t} + A v_t (2\pi)^{-1} e^{-\omega_t t/\sqrt{2}} \sin \left(\frac{\pi}{4} + \frac{\omega_t t}{\sqrt{2}} \right) . \quad (2.10)$$

With A and B as defined in (2.1) and with (2.7),

$$\gamma_{xx}(t) = \sqrt{2} \sigma_t^2 e^{-\omega_t t/\sqrt{2}} \sin \left(\frac{\pi}{4} + \frac{\omega_t t}{\sqrt{2}} \right) + \sigma_s^2 e^{-\omega_s t} . \quad (2.11)$$

The autocorrelation function is defined as

$$\rho_{xx}(t) = \gamma_{xx}(t)/\gamma_{xx}(0) . \quad (2.12)$$

In this case,

$$\gamma_{xx}(0) = \sigma_t^2 + \sigma_s^2 . \quad (2.13)$$

An Example

Using parameter estimates from tracking run number 75A of the CLGP
OT 1 Tracking Tests,

(2-3)

$$v_t = 0.7 \text{ hz} \quad \omega_t = 4.398 \text{ r/s}$$

$$v_s = 3 \text{ hz} \quad \omega_s = 18.850 \text{ r/s}$$

$$\sigma_t = 0.23 \text{ m} \quad (\text{at } 3 \text{ km range})$$

$$\sigma_s = 0.165 \text{ m}$$

$$\sigma_t^2 / (\sigma_t^2 + \sigma_s^2) = 0.6586$$

$$\sigma_s^2 / (\sigma_t^2 + \sigma_s^2) = 0.3414$$

$$\rho_{xx}(t) = 0.9314 \exp(-3.11t) \sin(0.7854 + 3.11t)$$

$$+ 0.3414 \exp(-18.85t). \quad (2.14)$$

This result is compared with the experimental estimates in Figure 2.

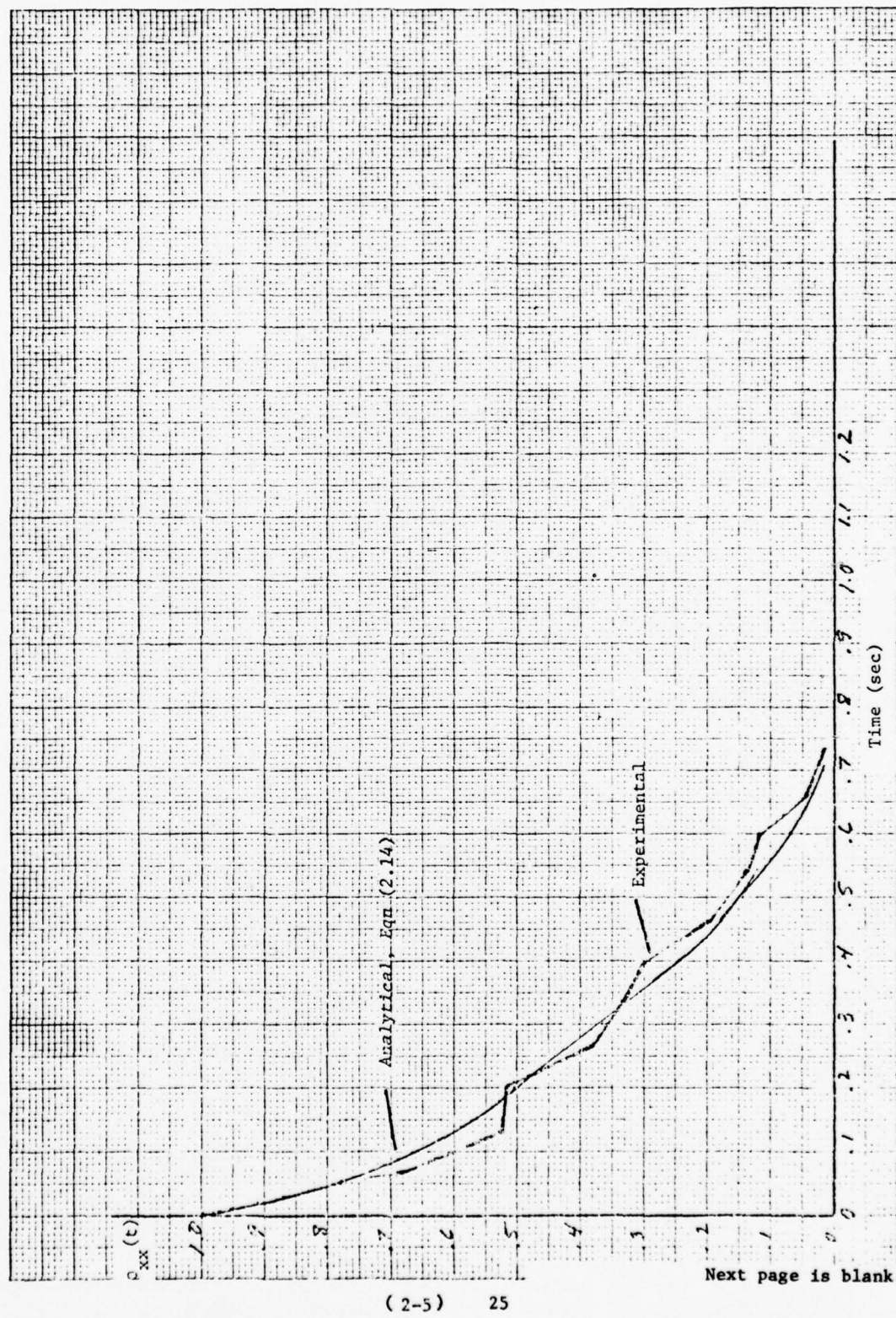


Figure 2. Autocorrelation Function for Run 75A--Analytic Versus Experimental

ANNEX 3

DIGITAL COMPUTER IMPLEMENTATION FOR THE FIRST-ORDER COMPONENT OF THE SPOT MOTION ERROR

Marginal statistics for the first-order process are assumed gaussian. However, for brevity the word "gaussian" is often omitted in describing the process. One implements a first-order, continuous (or, analog) stochastic process with a first-order digital filter having a discrete, mean-zero gaussian white noise input. The design of the filter is based upon the assumption that the continuous-time process is being time sampled.

Continuous-time (Analog) Processes.

The following first-order transfer function $H'(s)$:

$$H'(s) = \frac{(B/2\pi)^{1/2} \omega_s}{s + \omega_s} \quad (3.1)$$

having a continuous, white noise input generates the autospectrum

$$[H'(\omega)]^2 = \frac{(B/2\pi)^2 \omega_s^2}{\omega^2 + \omega_s^2}, \quad (3.2)$$

as in equation (2.4) of Annex 2, where the autospectrum of the output is just the squared modulus:

$$[H'(\omega)]^2 = H'(j\omega) H'(-j\omega) \quad (3.3)$$

for a white noise input of unit variance.

For convenience a normalized version of (3.1) is employed such that gain is unity for s equal to zero:

$$\bar{H}(s) = \omega_s / (s + \omega_s) . \quad (3.4)$$

Attention to the variance of the input white noise is deferred until later.

Filter Design.

A time sampling of the continuous process characterized by (3.4) can be used as the basis of the digital implementation. The z-transform describing the digital implementation of (3.4) can be obtained by performing a bilinear transformation from the s-plane into the z-plane. (See Walsh [3.1] or Stanley [3.2]). The bilinear z-transform is taken by substituting

$$s = (z - 1)/(z + 1) \quad (3.5)$$

into (3.4).

To minimize distortion of the spectrum of the digital process relative to the equivalent analog process we use a warped analog cutoff frequency, a (instead of ω_s), where

$$a = \tan(\omega_s T/2) = \tan(\pi v_s T),^{**} \quad (3.6)$$

with sampling interval T and desired angular cutoff frequency ω_s or natural cutoff frequency v_s .

Using the warped cutoff frequency, the digital transfer function^{*} is

$$H_z(z) = \frac{a}{\frac{z - 1}{z + 1} + a} . \quad (3.7)$$

* The digital transfer function is the ratio of the z-transforms of output to input of a digital filter.

[3.1] Walsh, P. J., A Study of Digital Filters, AD710381, Naval Postgraduate School, Monterey, CA., Dec 1969.

[3.2] Stanley, W. D. Digital Signal Processing, Reston Pub. Co., Inc., Reston, VA., c. 1975.

**This is a normalized version of the warping transformation of frequency required by the bilinear transformation. Normalization is achieved by division by $2/T$.

The useful (canonical) form of (3.7) is, after manipulation,

$$H_z(z) = \frac{a_0(1 + z^{-1})}{1 + bz^{-1}} , \quad (3.8a)$$

with

$$\begin{aligned} a_0 &= a/(a + 1) \\ b &= (a - 1)/(a + 1). \end{aligned} \quad (3.8b)$$

Remembering that z^{-1} is the backspace operator, implementation of the desired digital filter follows directly from (3.8). Notationally, let the noise input to the filter at time index t be n_t and the output at t be x_t , with t integer.

Then,

$$x_t + bx_{t-1} = a_0 n_t + a_0 n_{t-1} \quad (3.9)$$

or

$$x_t = a_0 n_t + a_0 n_{t-1} - bx_{t-1} . \quad (3.10)$$

Since the desired output spectrum requires a white noise input,

$$\begin{aligned} E[n_t n_{t-k}] &= 0 , k \neq 0 \\ &= \sigma_n^2 , k = 0. \end{aligned} \quad (3.11)$$

Variance Ratio of Output to Input.

In selecting the value of noise variance of the input to yield a particular output variance, it is necessary to know the ratio of output to input variance of the filter. In the following development an expression for this ratio will be derived. It will be useful to employ the following

notation for the covariance function:

$$\gamma_{xx}(k) = E[x_t x_{t-k}]. \quad (3.12)$$

In this notation, we desire

$$\gamma_{xx}(0)/\sigma_n^2 \text{ or } \gamma_{xx}(0)/\gamma_{nn}(0).$$

Taking the mathematical expectation of the product of n_t with both sides of (3.10) yields

$$E[x_t n_t] = a_o \sigma_n^2, \quad (t \text{ integer}), \quad (3.13)$$

since

$$E[n_t n_{t-1}] = 0$$

and

$$E[n_t x_{t-1}] = 0.$$

Similarly, taking the expectation of the product of n_{t-1} with both sides of (3.10) yields

$$E[x_t n_{t-1}] = a_o(1 - b) \sigma_n^2. \quad (3.14)$$

After squaring both sides of (3.10) and taking the mathematical expectation,

$$\begin{aligned} \gamma_{xx}(0) &= E[x_t^2] = E[a_o^2 n_t^2 + 2 a_o^2 n_t n_{t-1} - 2 a_o b n_t x_{t-1} - 2 a_o b n_{t-1} x_{t-1} \\ &\quad + a_o^2 n_{t-1}^2 + b^2 x_{t-1}^2]. \end{aligned} \quad (3.15)$$

With (3.13) and (3.14),

$$\gamma_{xx}(0)/\gamma_{nn}(0) = 2 a_o^2/(1 + b). \quad (3.16)$$

Alternatively, with (3.8b) ,

$$\gamma_{xx}(0)/\gamma_{nn}(0) = a/(a + 1) . \quad (3.17)$$

This is the desired result.

Summary.

In summary, to simulate a first-order, mean-zero process x_t having a desired cutoff frequency ν_s and standard deviation σ_s , one can employ the digital filter given by (3.10) with a gaussian, white noise input n_t having standard deviation given by

$$\begin{aligned} \sigma_n &= [\gamma_{nn}(0)/\gamma_{xx}(0)]^{1/2} \sigma_s \\ \sigma_n &= [(a + 1)/a]^{1/2} \sigma_s , - \end{aligned} \quad (3.18)$$

with a given by (3.6) and filter constants given by (3.8b).

ANNEX 4

DIGITAL COMPUTER IMPLEMENTATION FOR THE SECOND-ORDER COMPONENT OF THE SPOT MOTION ERROR

Analysis of a variety of man-operated trackers, such as those reported in [3], indicates that the marginal probability distribution function for the tracking component of laser spot motion is adequately described as gaussian. Additional experience with tracking records of this type indicates that a second-order dynamical system characterizes the tracking error. For most human trackers a good digital simulation of the mean-zero portion of the tracking error is obtained by filtering gaussian white noise with a second-order, low-pass Butterworth filter. As in Annex 3, the design of the digital filter is based upon the assumption that the continuous-time (analog) process is being time sampled.

Continuous-time (Analog) Processes.

The following transfer function describes a second-order analog process with analog corner frequency ω_a and damping constant ζ :

$$H_t(s) = \frac{\omega_a^2}{s^2 + 2\zeta \omega_a s + \omega_a^2} \quad (4.1)$$

Specifically for low-pass Butterworth filters $\zeta = 1/\sqrt{2}$ and

$$H_t(s) = \frac{\omega_a^2}{s^2 + \sqrt{2} \omega_a s + \omega_a^2} \quad (4.2)$$

The digital transfer function^{*} associated with (4.2) is created by mapping from the s-plane into the z-plane using the bilinear z-transform.

*The digital transfer function is the ratio of the z-transforms of output to input sequences of a digital filter.

(See Walsh, P. J., Op Cit [3.1]). The bilinear z-transform is taken by substituting

$$s = (z - 1)/(z + 1) \quad (4.3)$$

in (4.2). Thus,

$$\begin{aligned} H_z(z) &= H_t \left(\frac{z - 1}{z + 1} \right) \\ H_z(z) &= \frac{\omega_a^2 (z + 1)^2}{(z - 1)^2 + \sqrt{2} \omega_a (z - 1)(z + 1) + \omega_a^2 (z + 1)^2}. \end{aligned} \quad (4.4)$$

Reduction of $H_z(z)$ to the form

$$\frac{a_0 + a_1 z^{-1} + a_2 z^{-2}}{1 + b_1 z^{-1} + b_2 z^{-2}} \quad (4.5)$$

implies the digital filter, since z^{-1} is equivalent to a unit backspace operator. The coefficients in (4.5) are given by

$$a_0 = a_2 = \omega_a^2/D$$

$$a_1 = 2 a_0$$

$$b_1 = 2(\omega_a^2 - 1)/D$$

$$b_2 = (\omega_a^2 - \sqrt{2} \omega_a + 1)/D$$

with

$$D = \omega_a^2 + \sqrt{2} \omega_a + 1. \quad (4.6)$$

Notationally, let the noise input to the filter at time index t be n_t and the output at t be x_t , with t an integer. Then, from (4.5),

$$x_t + b_1 x_{t-1} + b_2 x_{t-2} = a_0 n_t + a_1 n_{t-1} + a_2 n_{t-2}. \quad (4.7)$$

Since the analog angular frequency ω_a associated with the bilinear transformation is "warped" or distorted relative to the desired digital cutoff angular frequency ω_t , we employ the relationship between these parameters:

$$\omega_a = \tan(\omega_t T/2)$$

or

$$\omega_a = \tan(\pi v_t T), \quad (4.8)$$

where T is the sampling period.

Parenthetically, note that a change in the sampling period, for a fixed digital cutoff frequency, would change ω_a and, by (4.6), would change the coefficients of the digital filter.

In operation, the filter arithmetic is performed as follows:

$$x_t = a_0 n_t + a_1 n_{t-1} + a_2 n_{t-2} - b_1 x_{t-1} - b_2 x_{t-2}, \quad (4.9)$$

with $t = 3, 4, \dots$

The filter is initialized by assigning $x_1 = x_2 = 0$, their mean values; and, then, cycling through a sufficient set of inputs to remove the effect of the initialization transient.

The form of (4.9) is referred to in the statistical literature, eg [4.1] and [4.2]^{*} as a mixed autoregressive, moving average model since the output x_t depends upon past values of the output -- x_{t-1} and x_{t-2} -- as

* [4.1] Box, G. E. P. and Jenkins, G. M., Time Series Analysis: Forecasting and Control, Holden-Day, San Francisco, c. 1970.

[4.2] Jenkins, G. M. and Watts, D. G., Spectral Analysis And Its Applications, Holden-Day, San Francisco, c. 1969.

well as upon (moving average) terms in the input -- n_t and n_{t-1} .

For the required autospectrum of x_t , n_t must be white. Thus,

$$\begin{aligned} E[n_t n_{t-k}] &= 0, k \neq 0 \\ &= \sigma_n^2, k = 0. \end{aligned} \quad (4.10)$$

Furthermore, future values of the input are uncorrelated with the present value of the output, ie,

$$E[n_{t+k} x_t] = 0, k > 0. \quad (4.11)$$

Ratio of Output to Input Variances.

In selecting the value of noise (input) variance to yield a particular output variance, it is necessary to know the ratio of output to input variances of the filter. An expression for this ratio will be derived. We employ a notation used by Jenkins [4.20] for, respectively, the autocovariance and crosscovariance functions:

$$\begin{aligned} \gamma_{xx}(k) &= E[x_t x_{t-k}] \\ \gamma_{xn}(k) &= E[x_t n_{t-k}]. \end{aligned} \quad (4.12)$$

In this notation, one desires

$$\gamma_{xx}(0)/\sigma_n^2 \text{ or } \gamma_{xx}(0)/\gamma_{nn}(0).$$

This result is obtained from (4.7) by successive multiplication of both sides by x_{t-1} , n_t , and n_{t-1} ; and, then, by taking the mathematical expectation on both sides in all equations. This produces:

$$\gamma_{xx}(1) = -b_1 \gamma_{xx}(0) - b_2 \gamma_{xx}(1) + a_1 \gamma_{xn}(0) + a_2 \gamma_{xn}(1)$$

and

$$\gamma_{xn}(0) = a_0 \sigma_n^2$$

$$\gamma_{xn}(1) = (a_1 - b_1 a_o) \sigma_n^2 .$$

Thus,

$$b_1 \gamma_{xx}(0) + (1 + b_2) \gamma_{xx}(1) = \\ [a_o a_1 + a_2 (a_1 - b_1 a_o)] \sigma_n^2 . \quad (4.13)$$

After squaring both sides of (4.9) and taking expected values, one obtains

$$(1 - b_1^2 - b_2^2) \gamma_{xx}(0) - 2 b_1 b_2 \gamma_{xx}(1) = \\ \sigma_n^2 [-2 a_o a_1 b_1 - 2 a_o a_2 b_2 - 2 a_2 b_1 (a_1 - b_1 a_o) + a_o^2 + a_1^2 + a_2^2] . \quad (4.14)$$

One can solve (4.13) and (4.14) for the desired variance ratio.

$$\gamma_{xx}(0)/\gamma_{nn}(0) = \frac{C_1 B_2 - B_1 C_2}{A_1 B_2 - B_1 A_2} , \quad (4.15a)$$

with

$$A_1 = b_1$$

$$A_2 = 1 - b_1^2 - b_2^2$$

$$B_1 = 1 + b_2$$

$$B_2 = -2 b_1 b_2$$

$$C_1 = a_o a_1 + a_2 (a_1 - b_1 a_o)$$

$$C_2 = -2 a_o a_1 b_1 - 2 a_o a_2 b_2 - 2 a_2 b_1 (a_1 - b_1 a_o) + a_o^2 + a_1^2 + a_2^2 . \quad (4.15b)$$

For numerical stability the denominator of the r.h.s. of (4.15a) must, of course, be non-zero. This implies that the parameters b_1 and b_2 must

lie within the region defined by:

$$|b_2| < 1$$

$$b_1 - b_2 < 1$$

and

$$b_1 + b_2 > -1.$$

This requirement is equivalent to the statement that the poles of (4.5) lie outside the unit circle. See Box, Op Cit, [4.1]. In practice, stability requirements are satisfied for the problem of modeling human tracker error using sampling rates of 10 or 20 hertz.

Summary.

To simulate the second-order, mean-zero component of a stochastic process having the desired cutoff frequency ν_t and standard deviation σ_t one can employ the digital filter given by (4.9) with a mean-zero, gaussian white-noise input n_t hav'ng a standard deviation given by

$$\sigma_n = [\gamma_{nn}(0)/\gamma_{xx}(0)]^{1/2} \sigma_t , \quad (4.16)$$

with variance ratio given by (4.15) and with filter coefficients given by (4.6).

ANNEX 5

AUTOSPECTRA OF THE DIGITAL ERROR PROCESSES

First Order Component

From the digital transfer function of the first-order process (equation (3.8a)),

$$H_z(z) = \frac{a_o(1+z^{-1})}{1+bz^{-1}} , \quad (5.1)$$

and with the following mapping into the frequency domain:

$$z = e^{j\omega T} = e^{j2\pi\nu T} , \quad (5.2)$$

the squared modulus

$$H_1^2(\nu) = H_z(e^{j2\pi\nu T}) H_z(e^{-j2\pi\nu T})$$

is

$$H_1^2(\nu) = \frac{2 a_o^2 (1 + \cos 2\pi\nu T)}{1 + b^2 + 2b \cos 2\pi\nu T} , \quad (5.3)$$

with ν defined over positive frequencies from zero to the Nyquist frequency $\nu_f = 1/(2T)$.

The results in (5.1) and (5.3) were derived from a normalized analog transfer function having unity gain at frequency zero. Consequently, $H_1^2(0) = 1$. Then, the autospectrum of the first-order digital component, $\Gamma_{xx}(\nu)$, is given by

$$\Gamma_{xx}(\nu) = H_1^2(\nu) \Gamma_{nn}(\nu) , \quad (5.4)$$

where $\Gamma_{nn}(\nu)$ is the autospectrum of the digital white noise (input) process, given by

(5-1)

$$\Gamma_{nn}(v) = v_f^{-1} \sigma_n^2, \quad 0 \leq v \leq v_f, \quad (5.5)$$

or, from (3.18),

$$\Gamma_{nn}(v) = 2T \sigma_s^2 (a+1)/a \quad (5.6a)$$

or

$$\Gamma_{nn}(v) = \frac{2T(1+b)}{2 a_o^2} \sigma_s^2, \quad 0 \leq v \leq v_f. \quad (5.6b)$$

The noise spectrum Γ_{nn} is comparable to the gain constant B in (1.10).

As T approaches zero Γ_{nn} approaches B .

Example

It is interesting to compare the value of the first-order component autospectrum for the analog process (equation (1.6)) with that for the equivalent digital implementation. To this end, take the parameters of the example given previously in Annex 1: $v_s = 3$ hz, $\sigma_s = 0.165$ m. Assuming that the sampling rate ($1/T$) of the analog process is 20 hz,

$T = 0.05$ sec, and, by (3.6),

$a = 0.509525$.

From (3.8b),

$$a_o = 0.337540$$

$$b = -0.324920 .$$

Then, (5.3) becomes

$$H_1^2(v) = \frac{0.227866 (1 + \cos 0.314159v)}{1.1055728 - 0.649839 \cos 0.314159v}, \quad (5.7)$$

This result is compared with that of the corresponding analog process in Table 2. Additionally, squared modulii for other sampling rates are displayed in Table 2.

TABLE 2. COMPARISON OF THE ANALOG AND DIGITAL SQUARED MODULII OF THE FIRST-ORDER ERROR PROCESS

| v (hz) | $H_s^2(v)$ analog, $B=1$ | $H_1^2(v)$, digital at sampling rate: | | |
|--|-----------------------------|--|-----------------------|-----------------------|
| | | 20 hz | 40 hz | 80 hz |
| 0.0 | 1.0000 | 1.0000 | 1.0000 | 1.0000 |
| 0.3 | 0.9901 | 0.9915 | 0.9904 | 0.9902 |
| 0.5 | 0.9730 | 0.9767 | 0.9739 | 0.9732 |
| 1.0 | 0.9000 | 0.9119 | 0.9030 | 0.9007 |
| 1.5 | 0.8000 | 0.8183 | 0.8045 | 0.8011 |
| 2.0 | 0.6923 | 0.7109 | 0.6968 | 0.6934 |
| 3.0 | 0.5000 | 0.5000 | 0.5000 | 0.5000 |
| 4.0 | 0.3600 | 0.3297 | 0.3531 | 0.3583 |
| 6.0 | 0.2000 | 0.1205 | 0.1817 | 0.1955 |
| 8.0 | 0.1233 | 0.0267 | 0.0984 | 0.1171 |
| 10.0 | 0.0826 | 0.0000 | 0.0545 | 0.0755 |
| $\Gamma_{nn}(v) \text{ (m}^2/\text{hz)}$ | $5.777 \cdot 10^{-3}$ | $8.066 \cdot 10^{-3}$ | $7.031 \cdot 10^{-3}$ | $6.431 \cdot 10^{-3}$ |

As noted from Table 2, the squared modulii of the analog and digital processes are in excellent agreement over the interval ($0 \leq v < v_f/2$). For frequencies within the interval ($v_f/2 \leq v \leq v_f$) and, particularly at the upper end of this interval, the autospectrum of the digital process departs significantly from that of the corresponding analog. Since there is no spectral content for the digital realizations above v_f , ie, all of the variance of the digital process must occur at frequencies below v_f , the values of the digital autospectrum exceed those of the analog having the same variance for low frequencies. Thus, the autospectrum of a digital process produced by a low sampling rate (and low v_f) will display substantial distortion relative to that of the corresponding analog process. This point is illustrated in Figure 3 in which different digital autospectra of the first-order stochastic process are compared to a corresponding analog auto-spectrum.

Of course, if the contribution of the first-order process to the total spot motion variance is small, this distortion may be acceptable. However, if fidelity to the corresponding analog process is desired, a general rule might be that the sampling rate used in generating the process digitally should be 20 to 30 times the corner frequency. Naturally, the dynamical response of the system accepting this first-order noise is also a consideration in selecting a sampling generation rate.

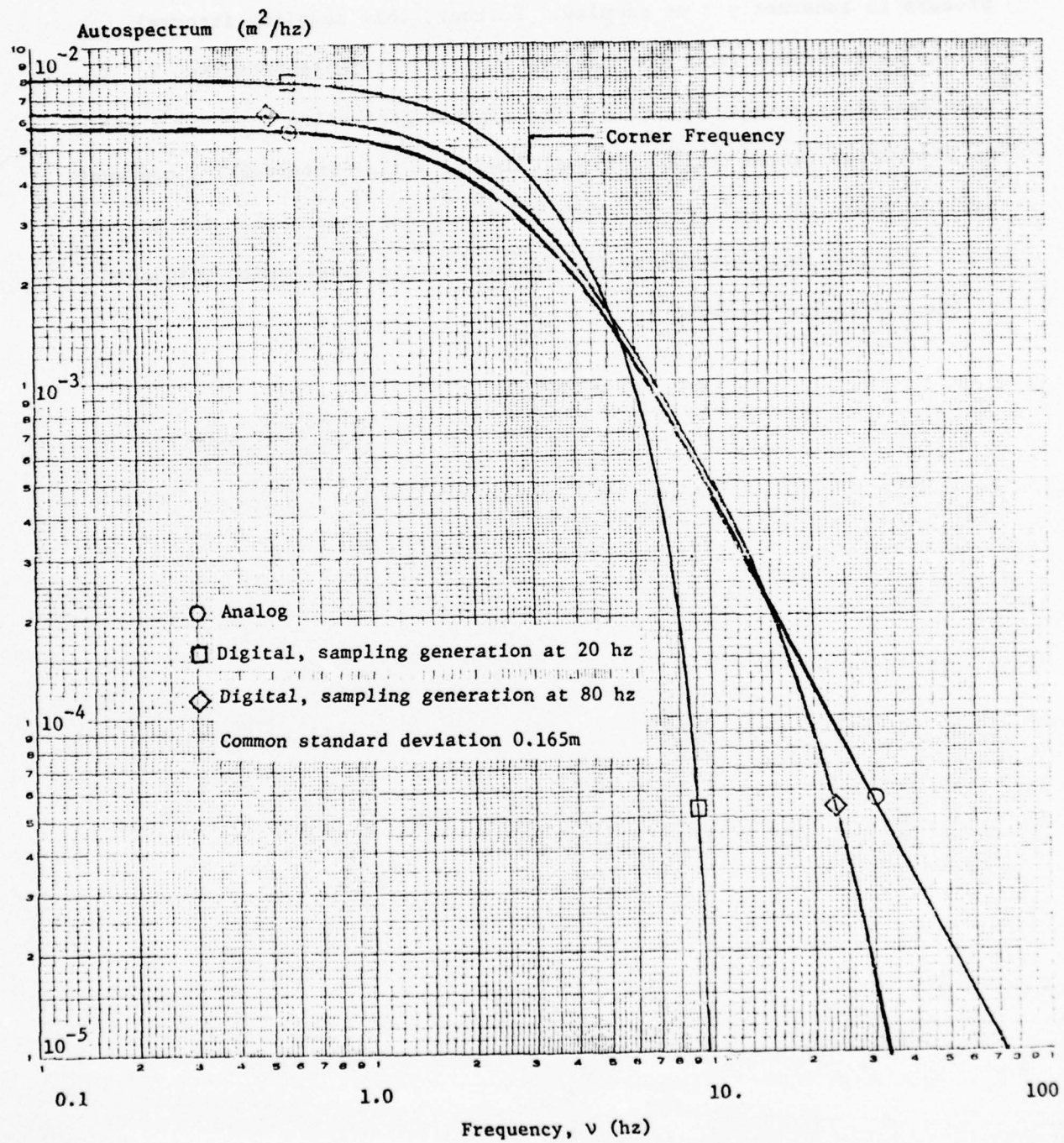


Figure 3. Comparison of the First-Order Autospectra for the Analog and Corresponding Digital Processes

(5-5)

Generally the dynamic components of a signal such as laser spot position are viewed only at discrete points in time, namely when the pulsed laser flashes. Thus, any spot motion due to a fundamentally continuous (analog) process is inherently time sampled. Further, this sampling interval T^* may be different from that used in the digital implementation, T . To quantitatively assess what effect the digital generation interval T has on the output series obtained by sampling at a time interval T^* , one must exploit some sampling theory. This theory is developed below for an ideal (delta-function) sampler and applied to the first-order component of the stochastic process.

The Transfer Function of a Time-Sampled Process

Whenever a stochastic process is sampled (or subsampled) the autospectrum of the sampled process may be substantially altered relative to the original process. This distortion will occur whenever the original process has an appreciable variance (or power) invested in frequencies (ν) above the Nyquist (or folding) frequency of the sampler. If the sampler is operating at a sampling rate $(T^*)^{-1}$, the folding frequency will be $\nu_f = (2T^*)^{-1}$ and variance in the original signal associated with $\nu > \nu_f$ will be confounded with the variance associated with ν for $0 \leq \nu < \nu_f$. In this section a theorem for ideal (point) samplers will be applied to several processes and examples will be offered to quantify the distortion accompanying sampling. In doing this, the author follows the notation and results of Kuo and Kaiser [5.1], p. 222 ff.

Notationally, let $f(nT^*)$ be the value of the original process evaluated at points in time: $t = nT^*$, with n an integer and T^* the constant sampling interval. Further, let $F(s)$ be the Laplace transform of the original process and let $F^*(s)$ be the Laplace transform of the sampled process, ie, of the discrete series resulting from sampling. Then, for zero initial conditions,

$$F^*(s) = \sum_{n=-\infty}^{\infty} F(s + jn2\pi/T^*) , \quad (5.8)$$

with $s = j\omega$ defined for $-\infty < \omega < \infty$.

[5.1] Kuo, F.F. and Kaiser J.F. Systems Analysis by Digital Computer, John Wiley and Sons, New York, c. 1966.

And,

$$F^*(j\omega) = F(j\omega) + \sum_{n=1}^{\infty} F(j(\omega+\omega_n)) + \sum_{n=1}^{\infty} F(j(\omega-\omega_n)), \quad (5.9a)$$

with

$$\omega_n = 2\pi n(T^*)^{-1} \quad (5.9b)$$

and

$$\omega = 2\pi\nu. \quad (5.9c)$$

Since the modulus of $F(j\omega)$ will generally decline with ω for values of ω greater than some value, say, ω^* , it will suffice to approximate F^* with a finite (and reasonably small) number of terms in the infinite sums.

Thus,

$$F^*(j\omega) \approx F(j\omega) + \sum_{n=1}^{n^*} F(j(\omega+\omega_n)) + \sum_{n=1}^{n^*} F(j(\omega-\omega_n)). \quad (5.10)$$

In evaluating the autospectrum of the sampled process it will be convenient to separately find the real and imaginary parts of each of the terms in $F^*(j\omega)$.

Then,

$$\begin{aligned} \text{Re } \{F^*(j\omega)\} &\approx \text{Re } \{F(j\omega)\} \\ &+ \sum_{n=1}^{n^*} \text{Re } \{F(j(\omega+\omega_n))\} \\ &+ \sum_{n=1}^{n^*} \text{Re } \{F(j(\omega-\omega_n))\}, \end{aligned} \quad (5.11)$$

and likewise for the imaginary part of $F^*(j\omega)$, $\text{Im } \{F^*(j\omega)\}$.

Finally, the autospectrum of the sampled process is proportional to

$$|F^*(j\omega)|^2 = [\text{Re } \{F^*(j\omega)\}]^2 + [\text{Im } \{F^*(j\omega)\}]^2. \quad (5.12)$$

As a particular application of the above results, take the first-order analog process, for which

$$F(s) = \omega_s (s + \omega_s)^{-1}. \quad (5.13)$$

(5-8)

In this case

$$F^*(j\omega) = \omega_s (j\omega + \omega_s)^{-1} + \omega_s \sum_{n=1}^{\infty} [j(\omega + \omega_n) + \omega_s]^{-1} + \omega_s \sum_{n=1}^{\infty} [j(\omega - \omega_n) + \omega_s]^{-1}. \quad (5.14)$$

Separating F^* into real and imaginary parts:

$$\begin{aligned} \operatorname{Re} \{F^*(j\omega)\} &= [(\omega/\omega_s)^2 + 1]^{-1} \\ &+ \sum_{n=1}^{\infty} [(\omega + \omega_n)^2/\omega_s^2 + 1]^{-1} \\ &+ \sum_{n=1}^{\infty} [(\omega - \omega_n)^2/\omega_s^2 + 1]^{-1} \end{aligned} \quad (5.15)$$

and

$$\begin{aligned} -\operatorname{Im} \{F^*(j\omega)\} &= (\omega/\omega_s) [(\omega/\omega_s)^2 + 1]^{-1} \\ &+ \sum_{n=1}^{\infty} ((\omega + \omega_n)/\omega_s) [(\omega + \omega_n)^2/\omega_s^2 + 1]^{-1} \\ &+ \sum_{n=1}^{\infty} ((\omega - \omega_n)/\omega_s) [(\omega - \omega_n)^2/\omega_s^2 + 1]^{-1}. \end{aligned} \quad (5.16)$$

This case has been evaluated for the following specific parameters:

$\omega_s = 1, 3 \text{ hz}$ and $T^* = 0.1, 0.05, 0.025 \text{ sec}$. The results are displayed in Figures 4 and 5.

A second example of the effect of sampling is the case in which a digital implementation of a first-order process is subsampled, ie, in which the sampling frequency $(T^*)^{-1}$ is a submultiple of the digital generation frequency T^{-1} . The digital process with transfer function $H_z(z)$ in equation (3.8a) will be the example taken here:

$$H_z(z) = \frac{a_0(1 + z^{-1})}{1 + bz^{-1}}. \quad (5.17)$$

With the mapping into the s-plane:

$$z = e^{sT}, \quad (5.18)$$

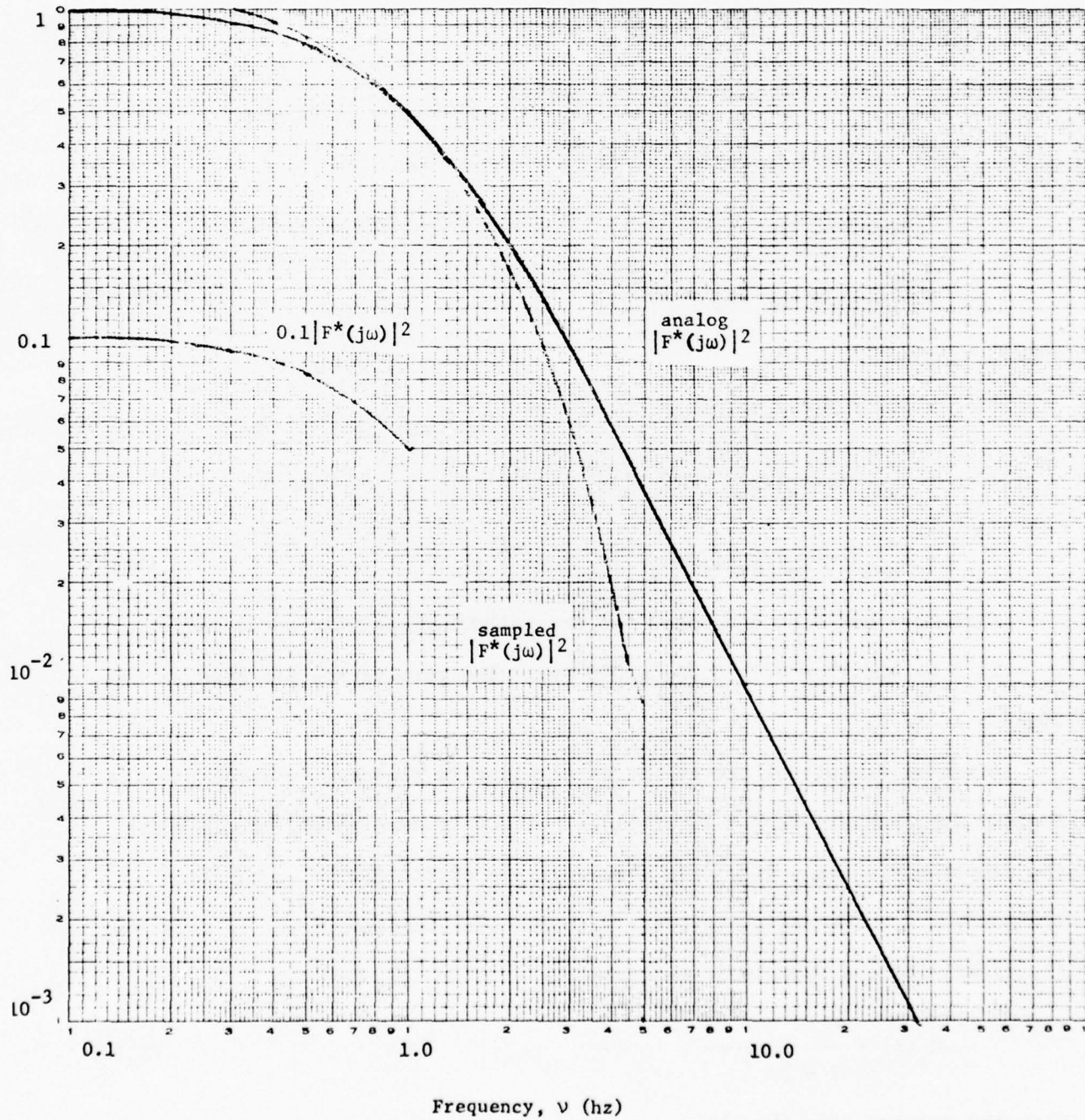


Figure 4. Comparison of a First-Order Analog Squared Modulus With the Squared Modulus of the Ideal Time-Sampled Series (Parameters: $v_s = 1$ hz, $T^* = 0.1$ sec)

(5-10)
48

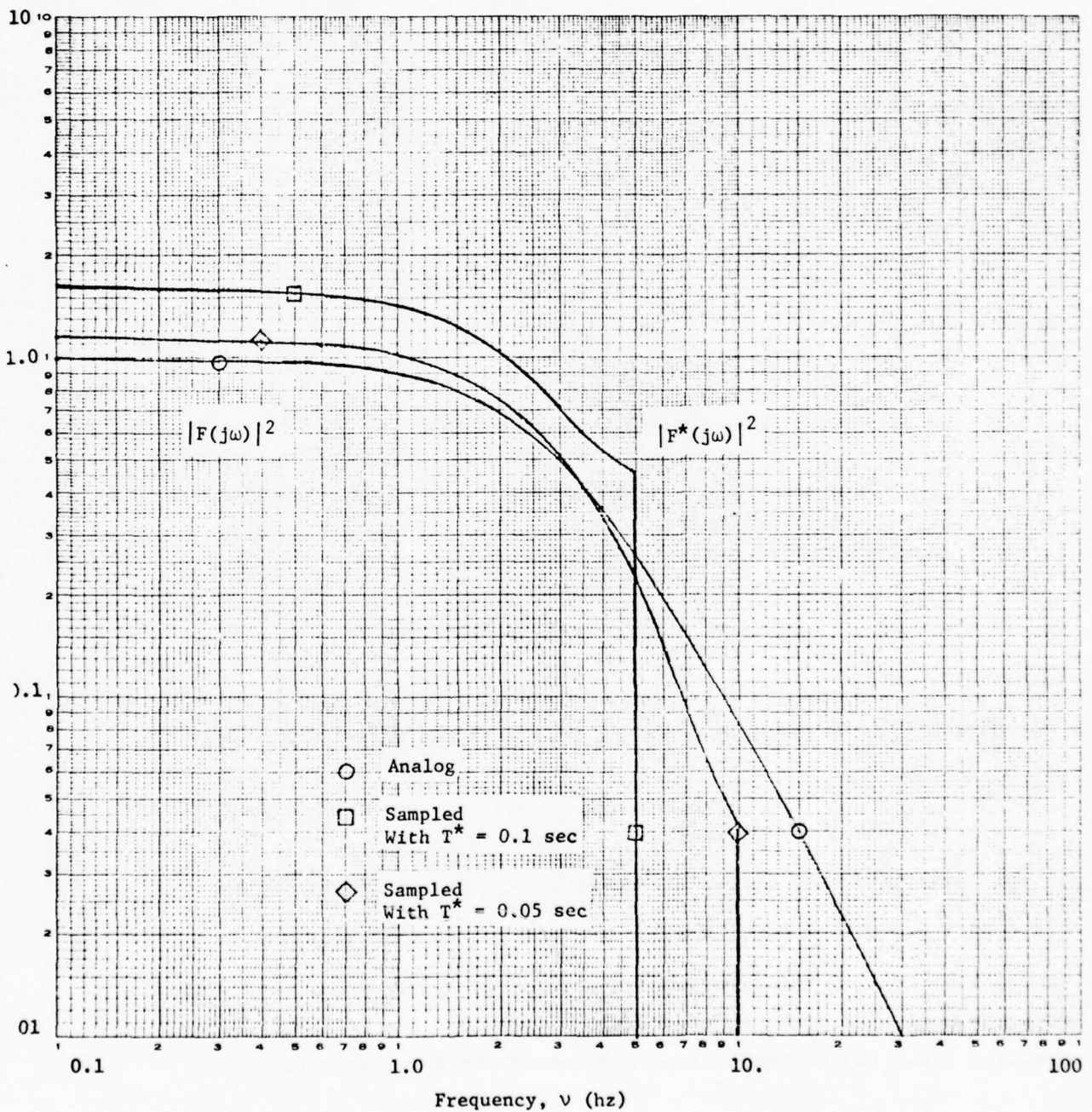


Figure 5. Comparison of a First-Order Analog Squared Modulus With the Squared Modulus of the Ideal Time-Sampled Series
 (Parameters: $\nu_s = 3$ hz, $T^* = 0.05, 0.1$ sec) (5-11)

$$F(s) = H_z(e^{sT}) = \frac{a_0(1 + e^{-sT})}{1 + b e^{-sT}} . \quad (5.19)$$

And,

$$F(j\omega) = \frac{a_0(1 + \exp(-j\omega T))}{1 + b \exp(-j\omega T)} , \quad (5.20a)$$

with (from (3.8b))

$$\begin{aligned} a_0 &= a/(a+1) \\ b &= (a-1)/(a+1) \\ a &= \tan(\pi v_s T) . \end{aligned} \quad (5.20b)$$

In this case,

$$\operatorname{Re}\{F(j\omega)\} = \frac{a_0(1+b)(1+\cos\omega T)}{1+b^2+2b\cos\omega T} \quad (5.21a)$$

and

$$-\operatorname{Im}\{F(j\omega)\} = \frac{a_0(1-b)\sin\omega T}{1+b^2+2b\cos\omega T} , \quad (5.21b)$$

for $-\pi \leq \omega T \leq \pi$; and when ωT is outside of this region, $F(j\omega)$ is identically zero.

Obviously, the sampling interval T^* must be an integral multiple of the generation interval T :

$$T^* = mT, m = 1, 2, 3 \dots$$

In this example $F^*(j\omega)$ is evaluated for $v_s = 3$ hz and $T = 0.025$ and $T = 0.05$ sec with $m = 2$. Results are plotted in Figures 6 and 7.

The autospectra for the time-sampled process in Figure 7 may be compared with the unsampled autospectra shown in Figure 3. The effect of sub-sampling order (m) on the squared modulus is shown in Table 3.

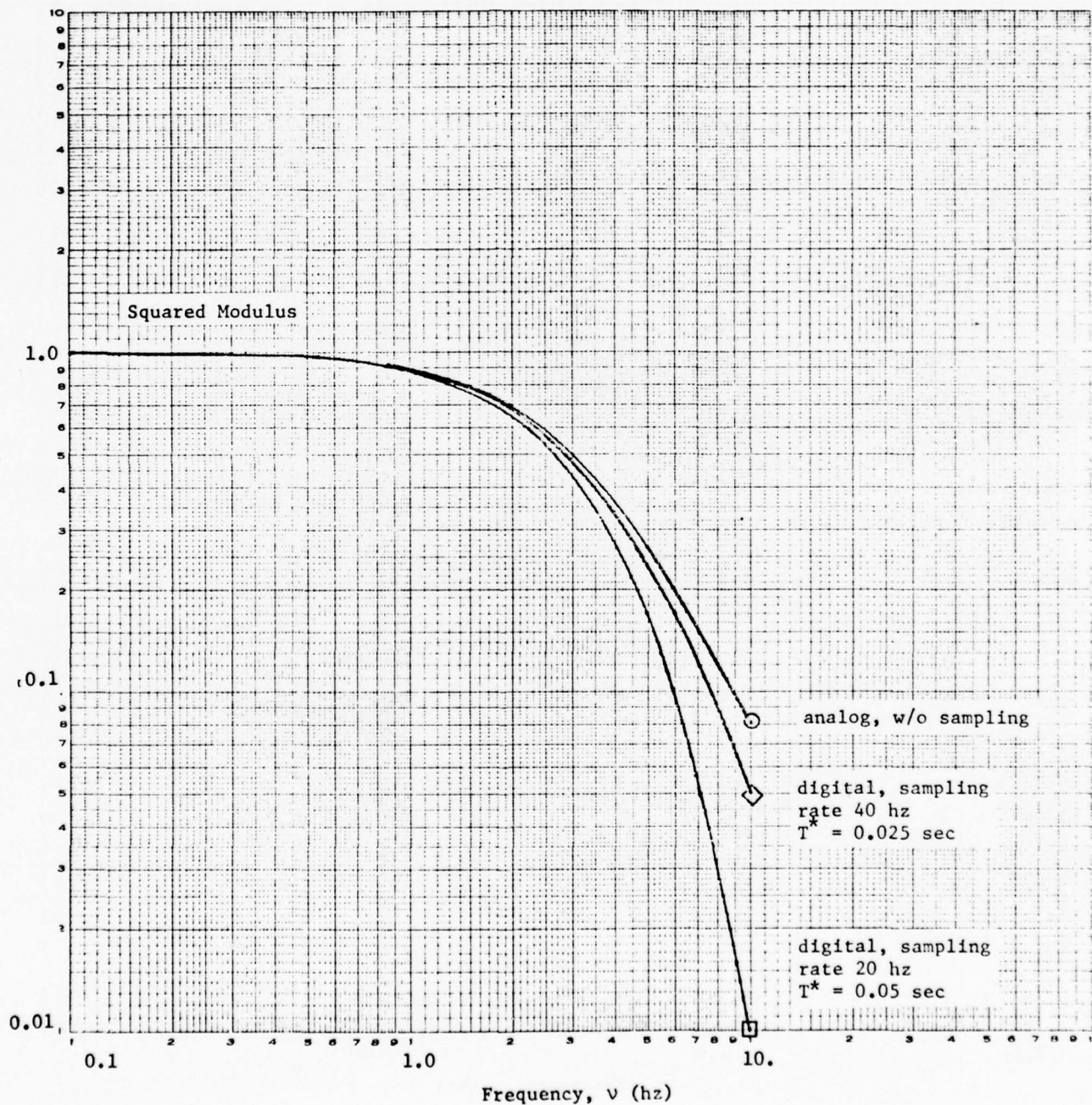


Figure 6. Comparison of Squared Modulii for Subsampled Digitally Generated First-Order Processes Having Different Sampling Rates
 (Parameters: $v_s = 3$ hz, $T = T^*/2$) (5-13)

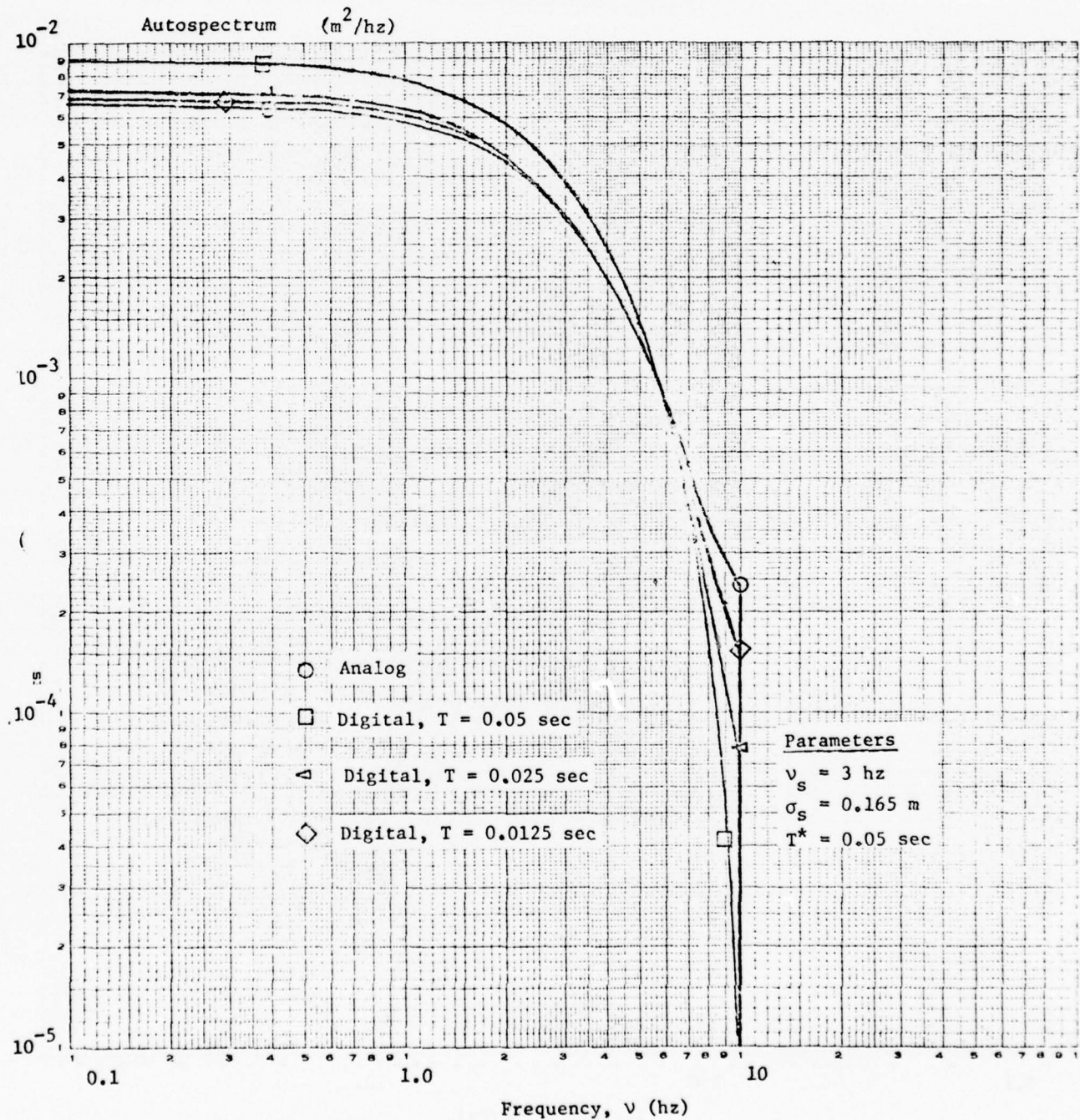


Figure 7. Comparison of the Autospectra of Time-Sampled Processes: Analog and Digital Implementations (Parameters: $v_s = 3 \text{ hz}$, $\sigma_s = 0.165 \text{ m}$, $T^* = 0.05 \text{ sec}$)

(5-14)

TABLE 3. EFFECT OF SUBSAMPLING ON THE SQUARED
MODULUS OF A DIGITAL IMPLEMENTATION OF A
FIRST-ORDER DYNAMIC PROCESS SAMPLED AT 20 Hz

Parameters: $v_s = 3 \text{ hz}$, $T^* = 0.05 \text{ sec}$

| v (hz) | digital $ F(j\omega) ^2$ with $T = T^*/m$ subsampling order m | | | |
|-----------|--|--------|--------|--------|
| | 1 | 2 | 3 | 4 |
| 0.1 | 0.9987 | 0.9987 | 1.0311 | 1.0537 |
| 0.2 | 0.9949 | 0.9950 | 1.0272 | 1.0497 |
| 0.3 | 0.9887 | 0.9887 | 1.0208 | 1.0432 |
| 0.4 | 0.9800 | 0.9801 | 1.0120 | 1.0342 |
| 0.5 | 0.9690 | 0.9692 | 1.0008 | 1.0229 |
| 0.6 | 0.9560 | 0.9562 | 0.9875 | 1.0093 |
| 0.7 | 0.9409 | 0.9412 | 0.9721 | 0.9937 |
| 0.8 | 0.9240 | 0.9440 | 0.9549 | 0.9762 |
| 1.0 | 0.8855 | 0.8861 | 0.9157 | 0.9363 |
| 1.2 | 0.8420 | 0.8430 | 0.8714 | 0.8913 |
| 1.5 | 0.7709 | 0.7724 | 0.7991 | 0.8177 |
| 2.0 | 0.6475 | 0.6500 | 0.6737 | 0.6901 |
| 2.5 | 0.5306 | 0.5342 | 0.5551 | 0.5694 |
| 3.0 | 0.4276 | 0.4323 | 0.4507 | 0.4632 |
| 3.5 | 0.3406 | 0.3463 | 0.3625 | 0.3735 |
| 4.0 | 0.2687 | 0.2753 | 0.2898 | 0.2995 |
| 4.5 | 0.2100 | 0.2174 | 0.2305 | 0.2392 |
| 5.0 | 0.1624 | 0.1704 | 0.1824 | 0.1902 |

Aside from the distortions in the autospectrum (and process dynamics) due to digital sampling, there are distortions in the spectral estimates created by the statistical techniques employed in analyzing time series data. These distortions are discussed below.

The Effect of Lag Window in the Estimated Autospectrum

In estimating an autospectrum from time series data, it is essential to provide a means of averaging or smoothing spectral estimates to insure stochastic convergence as the length of the series (or record) grows indefinitely large. For a single record, $x(t)$, the smoothing is efficiently done by applying a weight function or "lag window", $w(t)$, to the estimated autocovariance function, $\hat{\gamma}_{xx}(t)$, before taking the Fourier transform to form the smoothed autospectrum, $\hat{\Gamma}_{xx}(\omega)$. See Jenkins and Watts, 1968, Op Cit. Thus, for a continuous record of length t_e ,

$$\hat{\Gamma}_{xx}(\omega) = \frac{2}{\pi} \int_0^{t_e} \hat{\gamma}_{xx}(t) w(t) \cos \omega t dt. \quad (5.22)$$

Without applying a weight function to the theoretical autocovariance, and for an essentially infinite record, one would obtain the theoretical (unsmoothed) autospectrum:

$$\Gamma_{xx}(\omega) = \frac{2}{\pi} \int_0^{\infty} \gamma_{xx}(t) \cos \omega t dt. \quad (5.23)$$

Parenthetically, it is noted that the spectrum is often expressed in terms of the natural frequency v rather than the angular frequency ω . Then,

$$\begin{aligned} \Gamma'_{xx}(v) &= \Gamma_{xx}(\omega(v)) \left| \frac{d\omega}{dv} \right| \\ \Gamma'_{xx}(v) &= 2\pi \Gamma_{xx}(2\pi v). \end{aligned} \quad (5.24)$$

Altho smoothing is required to reduce the variance of the estimated auto-spectrum, it does create a distortion of the estimate $\hat{\Gamma}_{xx}(\omega)$ relative to $\Gamma_{xx}(\omega)$. It is the purpose of the developments of this section to quantify this distortion.

Two weight functions are frequently used in smoothing: one due to Bartlett--

$$w_B(t) = \begin{cases} 1 - t/\tau_m & , 0 \leq t \leq \tau_m \\ 0 & , t > \tau_m \end{cases}, \quad (5.25)$$

where τ_m is a lag parameter, and one due to Tukey--

$$w_T(t) = \frac{1}{2} (1 + \cos(\pi t/\tau_m)), \quad 0 \leq t \leq \tau_m \\ = 0 \quad , \quad t > \tau_m. \quad (5.26)$$

In the following analysis the simpler, Bartlett window is used. However, the effect shown on the estimated autospectrum is representative of several lag windows. Also in this analysis we take the estimated autocovariance function to be the theoretical autocovariance of a first-order analog process:

$\gamma_{xx}(t) = \gamma_{xx}(0) \exp(-\lambda t)$. Specifically, from the second term of (2.11), the autocovariance of the scintillation process is

$$\gamma_{xx}(t) = \sigma_s^2 e^{-\omega_s t} \quad (5.27)$$

Then, for the Bartlett weight function, the smoothed autospectrum is

$$\hat{\Gamma}_{xx}(\omega) = \frac{2\sigma_s^2}{\pi} \int_0^{\tau_m} \cos(\omega t) e^{-\omega_s t} (1 - t/\tau_m) dt. \quad (5.28)$$

$$\hat{\Gamma}_{xx}(\omega) = \frac{2\sigma_s^2}{\pi \omega_s} \int_0^{\omega_s \tau_m} \cos\left(\frac{\omega}{\omega_s} x\right) e^{-x} \left(1 - \frac{x}{\omega_s \tau_m}\right) dx. \quad (5.29)$$

From (1.10), the constant multiplier on the r.h.s. of (5.29) is $B/2\pi$.

$$\begin{aligned}\frac{2\pi}{B} \hat{\Gamma}_{xx}(\omega) &= \int_0^{\omega_s \tau_m} \cos\left(\frac{\omega}{\omega_s} x\right) e^{-x} dx \\ &\quad - \frac{1}{\omega_s \tau_m} \int_0^{\omega_s \tau_m} x e^{-x} \cos\left(\frac{\omega}{\omega_s} x\right) dx.\end{aligned}\quad (5.30)$$

After some manipulation,

$$\begin{aligned}\frac{2\pi}{B} \hat{\Gamma}_{xx}(\omega) &= \bar{\Gamma}_{xx}(\omega) + \alpha(\omega) \\ &\quad + e^{-\omega_s \tau_m} [\alpha(\omega) \cos \omega \tau_m + \beta(\omega) \sin \omega \tau_m],\end{aligned}\quad (5.31a)$$

where

$$\begin{aligned}\bar{\Gamma}_{xx}(\omega) &= (1 + (\omega/\omega_s)^2)^{-1} \\ \alpha(\omega) &= \omega_s \tau_m^{-1} (\omega_s^2 - \omega^2) (\omega_s^2 + \omega^2)^{-2} \\ \alpha(\omega) &= \frac{1 - (\omega/\omega_s)^2}{\omega_s \tau_m (1 + (\omega/\omega_s)^2)^2} \\ \beta(\omega) &= -2 \omega_s \tau_m^{-1} \omega (\omega_s^2 + \omega^2)^{-2} \\ \beta(\omega) &= -2 (\omega/\omega_s) (\omega_s \tau_m)^{-1} (\bar{\Gamma}_{xx}(\omega))^2.\end{aligned}\quad (5.31b)$$

Note that the normalized smoothed autospectrum $(2\pi/B) \hat{\Gamma}_{xx}$ approaches the unsmoothed function $\bar{\Gamma}_{xx}$ as τ_m grows infinite. Some numerical examples of $\hat{\Gamma}$ were evaluated for several values of the parameters v_s (or ω_s) and τ_m . Results are displayed in Figures 8 and 9. The effect of smoothing is to shift variance (or power) to lower frequencies and to introduce a damped oscillatory term. These distortions are not very significant for values of $v_s \tau_m$ greater than about 1.5.

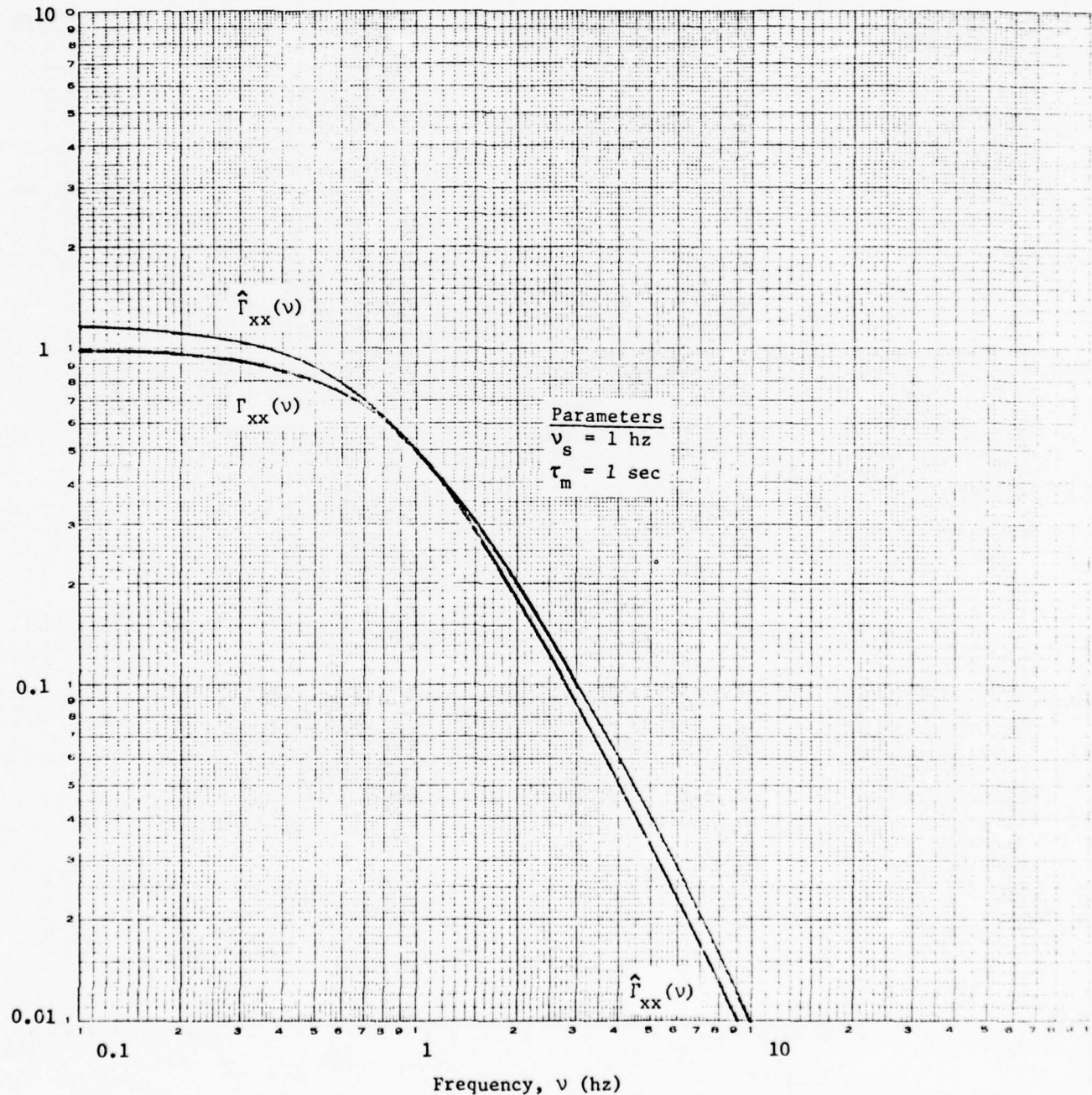


Figure 8. The Smoothed Autospectrum, $\hat{\Gamma}_{xx}(v)$, Due to a Bartlett Lag Window Applied to a First-Order Autocovariance With Associated Theoretical (Unsmoothed) Spectrum $\Gamma_{xx}(v)$, (Parameters: $v_s = 1 \text{ hz}$, $\tau_m = 1 \text{ sec}$) (5-19)

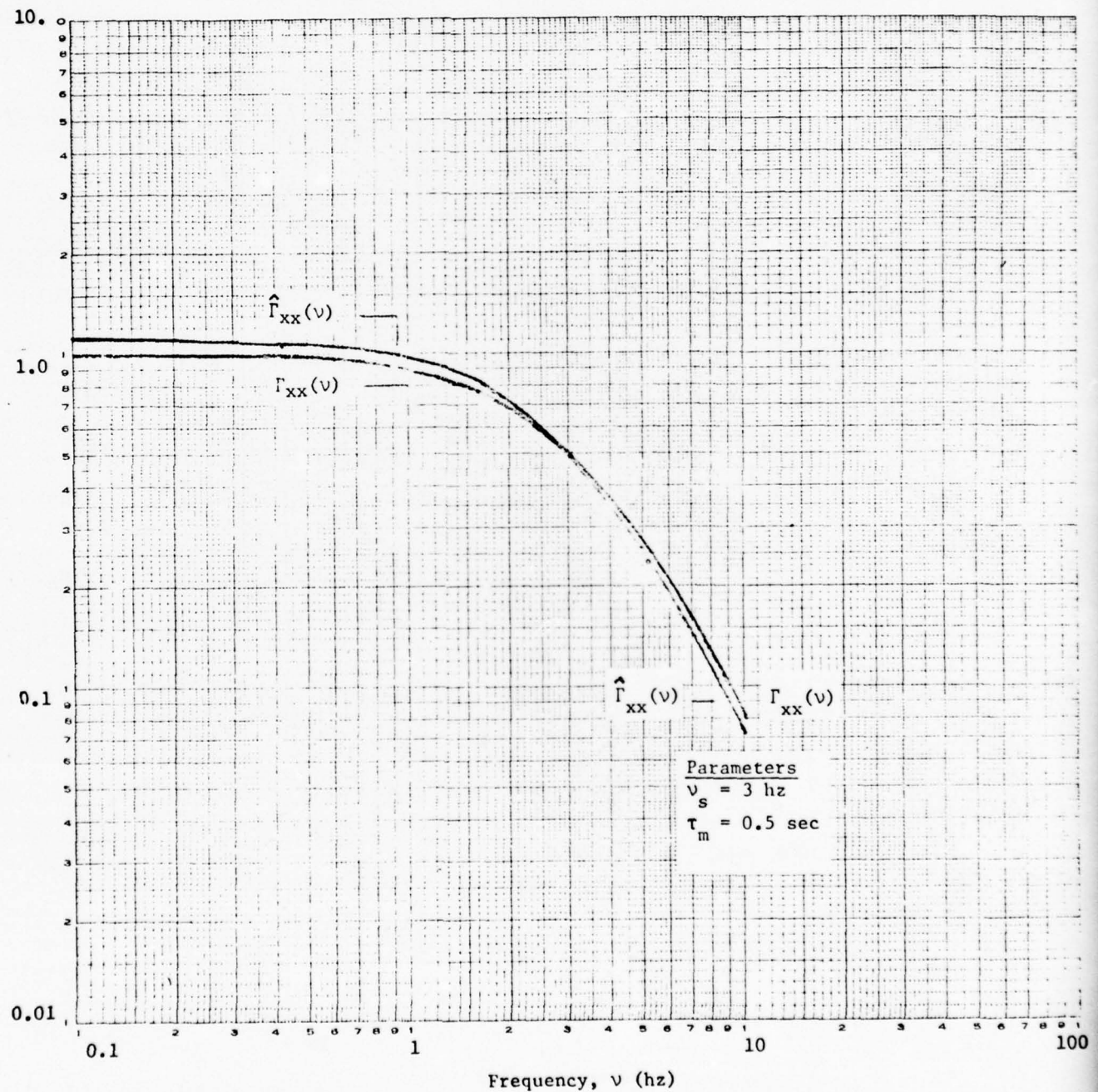


Figure 9. The Smoothed Autospectrum, $\hat{\Gamma}_{xx}(v)$, Due to a Bartlett Lag Window Applied to a First-Order Autocovariance With Associated Theoretical (Unsmoothed) Spectrum $\Gamma_{xx}(v)$

(Parameters: $v_s = 3$ hz, $\tau_m = 0.5$ sec) (5-20)

Second-Order Component

The digital transfer function used in describing the second-order, tracking component of the laser spot motion (equation (4.5)) is repeated here.

$$H_z(z) = \frac{a_0 + a_1 z^{-1} + a_2 z^{-2}}{1 + b_1 z^{-1} + b_2 z^{-2}} . \quad (5.32)$$

The autospectrum of the process is proportional to the squared modulus $|H_z(\exp(j\omega T))|^2$. Notationally,

$$H_2^2(\omega) = |H_z(e^{j\omega T})|^2 = |H_z(e^{j2\pi\nu T})|^2 , \quad (5.33)$$

with sampling generation interval T.

Using De Moivre's theorem,

$$e^{j\omega T} = \cos \omega T + j \sin \omega T , \quad (5.34)$$

with (5.32) and (5.33),

$$\begin{aligned} H_2^2(\omega) &= [(a_0 + a_1 \cos \omega T + a_2 \cos 2\omega T)^2 \\ &\quad + (a_1 \sin \omega T + a_2 \sin 2\omega T)^2] / \\ &\quad [(1 + b_1 \cos \omega T + b_2 \cos 2\omega T)^2 + (b_1 \sin \omega T + b_2 \sin 2\omega T)^2] . \quad (5.35) \end{aligned}$$

Using equation (4.6) and after some manipulation, (5.35) becomes

$$H_2^2(\omega) = \frac{\frac{\omega^4}{a} (3 + 4 \cos \omega T + \cos 2\omega T)}{3(\frac{\omega^4}{a} + 1) + 4(\frac{\omega^4}{a} - 1) \cos \omega T + (\frac{\omega^4}{a} + 1) \cos 2\omega T} , \quad (5.36)$$

where

$$\omega_a = \tan(\pi\nu_t T) . \quad (5.37)$$

Either (5.35) or (5.36) can be used to evaluate the squared modulus of the second-order dynamic component. Altho (5.36) has a simpler form than (5.35), computational experience using single-precision arithmetic on the IBM 360 series computers has demonstrated that (5.36) is somewhat more sensitive to truncation error than (5.35). In fact, it is noted

that generally all second-order transfer functions and squared modulii are more sensitive to loss of precision due to arithmetic truncation than are their first-order counterparts. When using IBM 360 computers it is recommended that double-precision arithmetic be used.

The above expressions for the second-order squared modulus are normalized so that $H_2^2(0) = 1$. To calculate the autospectrum, $\Gamma_{xx}(v)$, of the second-order (tracking) process, one employs:

$$\Gamma_{xx}(v) = H_2^2(2\pi v) \Gamma_{nn}(v), \quad (5.38)$$

where $\Gamma_{nn}(v)$ is the input noise spectrum to the second-order digital filter. The noise spectrum is a function of the sampling generation interval, T , and the variance of the tracking process, σ_t^2 :

$$\Gamma_{nn} = 2T \sigma_t^2 [\gamma_{nn}(0)/\gamma_{xx}(0)], \quad (5.39)$$

with the ratio of variances $\gamma_{nn}(0)/\gamma_{xx}(0)$

given by (4.15a).

As with the first-order process, it is useful to make numerical comparisons between the squared modulus of the digital implementation of the second-order (tracking) component and that of the corresponding analog process. The transfer function for a general second-order analog process, $H_t(s)$, is given by equation (4.1). The general squared modulus is, then,

$$H_t^2(j\omega) = 1/[(1 - (\omega/\omega_a)^2)^2 + 4\zeta^2(\omega/\omega_a)^2] \quad (5.40)$$

With the Butterworth assumption of $\zeta = 1/\sqrt{2}$ and with $\omega_a = 2\pi\nu_t$,

$$H_t^2(v) = 1/[1 + (v/v_t)^4], \quad (5.41)$$

as in equation (1.1) with $A = 1$.

The analog gain constant A (equation (1.5)) represents the analog input noise spectrum and is comparable with Γ_{nn} given by (5.39). In fact,

$$\lim_{T \rightarrow 0} \Gamma_{nn} = A. \quad (5.42)$$

Pursuing the example of Annex 1, with

$$v_t = 0.7 \text{ hz}$$

$$\sigma_t = 0.23 \text{ m}$$

$$T = 0.1 \text{ sec},$$

$$\omega_a = 0.219912, \text{ and from (5.36):}$$

$$\begin{aligned} H_2^2(v) &= 2.33879 \cdot 10^{-3} [3 + 4 \cos(0.62832v) \\ &\quad + \cos(1.25664v)]/[3.00716 \\ &\quad - 3.99064 \cos(0.62832v) + 1.002339 \cos(1.25664v)]. \end{aligned} \quad (5.43)$$

Numerical results from this expression and similar digital squared modulii calculated with $T = 0.05 \text{ sec}$ and 0.025 sec are compared with the analog squared modulus in Table 4. Spectral amplitudes for the noise are also shown in Table 4. Spectra are plotted in Figure 10.

TABLE 4. COMPARISON OF THE ANALOG AND DIGITAL SQUARED MODULII OF THE SECOND-ORDER (TRACKING) ERROR PROCESS

| v (hz) | analog $H_z^2(v)$ A=1 | $H_2^2(v)$ with T (sec): | | |
|---------------------------------------|-----------------------------|--------------------------|---------|---------|
| | | 0.025 | 0.05 | 0.10 |
| 0.1 | 1.000 | 1.000 | 1.000 | 1.000 |
| 0.2 | 0.993 | 0.993 | 0.993 | 0.994 |
| 0.3 | 0.967 | 0.967 | 0.968 | 0.969 |
| 0.4 | 0.904 | 0.904 | 0.905 | 0.907 |
| 0.5 | 0.793 | 0.794 | 0.794 | 0.799 |
| 0.6 | 0.649 | 0.650 | 0.650 | 0.653 |
| 0.7 | 0.500 | 0.500 | 0.500 | 0.500 |
| 0.8 | 0.370 | 0.369 | 0.368 | 0.365 |
| 1.0 | 0.194 | 0.193 | 0.191 | 0.183 |
| 1.2 | 0.104 | 0.103 | 0.101 | 0.092 |
| 1.5 | 0.0453 | 0.0447 | 0.0428 | 0.0357 |
| 2.0 | 0.0148 | 0.0144 | 0.0132 | 0.0089 |
| 3.0 | 0.00296 | 0.00275 | 0.00220 | 0.00070 |
| 5.0 | 0.00038 | 0.00031 | 0.00015 | 0.00000 |
| $\Gamma_{nn}(v)$ (m ² /hz) | 0.0680 | 0.0682 | 0.0685 | 0.0695 |

(5-23)

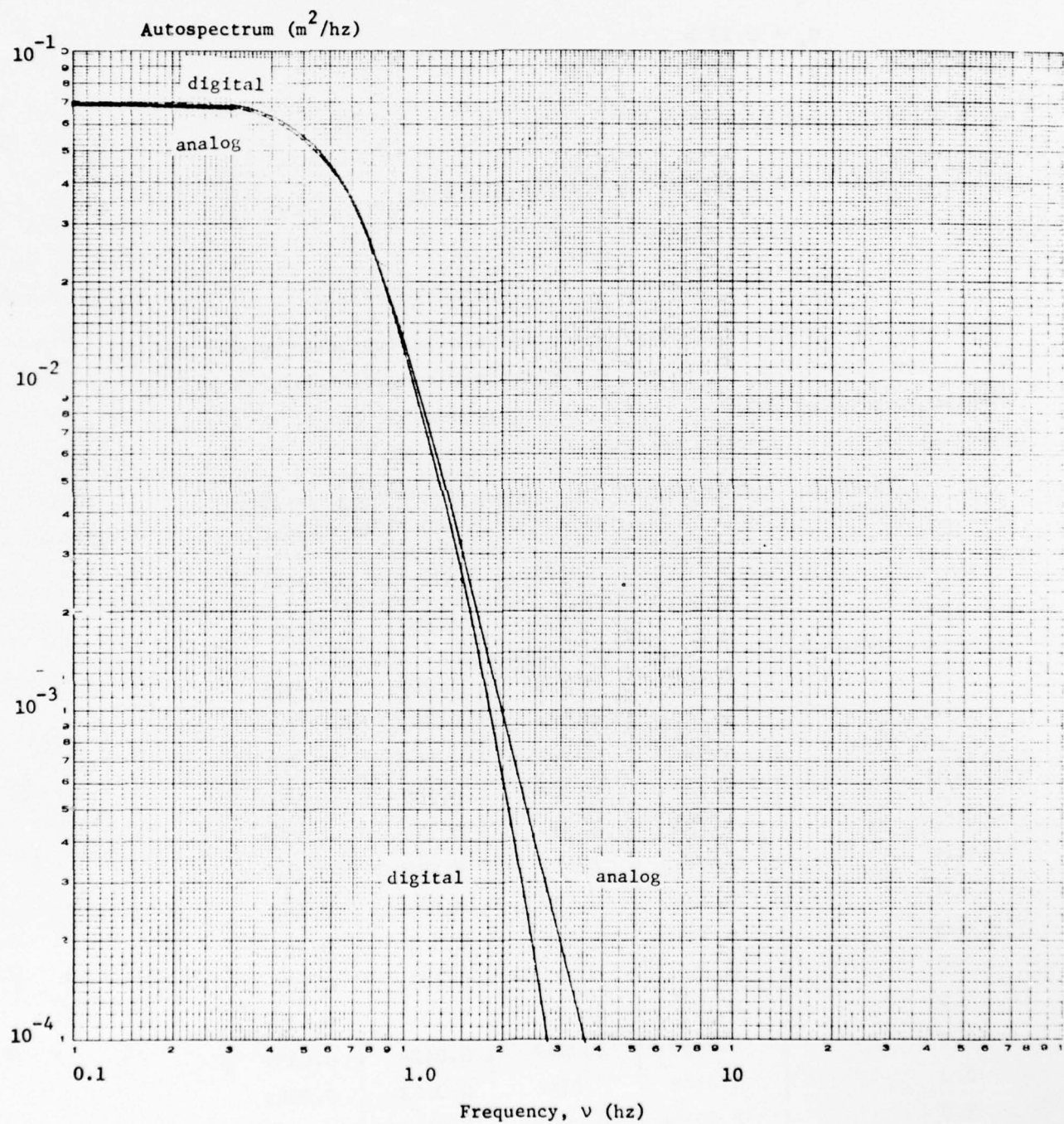


Figure 10. Autospectra of the Second-Order (Tracking) Process (Parameters:
 $v_t = 0.7 \text{ hz}$, $\sigma_t = 0.230 \text{ m}$, $T = 0.1 \text{ sec}$)

(5-24)

ATTACHMENT 1

REFERENCES

1. Memorandum for Record, AMSAR-SAM, 23 Jul 75, subject: Army-Navy Guided Projectile Effectiveness Study.
2. Technical Report, DRSAR-SAM, Report No. DRSAR/SA/N-51 (AD A032683), title: Distribution of Angle of Obliquity of Laser-Guided Projectiles With Respect to the Target at Impact.
3. Appendix G of Technical Report RG-75-29, AMSMI-RG, 18 Dec 74, report title: Analysis and Digital Simulation Models for CLGP: Martin Marietta Aerospace Design.
4. Letter, AMSAR-SA, 10 Dec 74, subject: Reduction and Analysis of CLGP-OT-1 Tracking Data.
5. Memorandum for Record, DRSAR-SAM, 11 Nov 76, subject: Proportion of Energy Spilled Over a Target During Tracking With a Laser Designator and Implications for Terminal Guidance.
6. Memorandum for Record, AMSAR-SAM, 16 Jan 76, subject: Laser Guidance Measurements Program.
 - 3.1 Walsh, P. J., A Study of Digital Filters, AD710381, Naval Postgraduate School, Monterey, CA., Dec 1969.
 - 3.2 Stanley, W. D. Digital Signal Processing, Reston Pub. Co., Inc., Reston, VA., c. 1975.
 - 4.1 Box, G. E. P. and Jenkins, G. M., Time Series Analysis: Forecasting and Control, Holden-Day, San Francisco, c. 1970.
 - 4.2 Jenkins, G. M. and Watts, D. G., Spectral Analysis and Its Applications, Holden-Day, San Francisco, c. 1969.

Next page is blank.

COST DIFFERENTIAL (COSDIF) PROBABILITIES

Next page is blank.

DRCAR-SAS

23 JAN 1977

MEMORANDUM FOR RECORD

SUBJECT: Cost Differential (COSDIF) Probabilities

1. The Systems Analysis Directorate was requested to develop ARMCOM's Cost Differential (COSDIF) Probabilities for both provisioning and replenishment type items. This MFR addresses the COSDIF probabilities as applied to replenishment items.
2. The COSDIF formula is used to determine if it is cost effective to stock an item when the expected yearly demand is 12 or less. Inputs to this formula include various costs and the probability that an item will have no demands in the next two years. ARMCOM is presently using the DODI 4140.42 probabilities (hard-coded in COSDIF) which were developed by the DoD from data supplied from one Army ICP and two DSA ICPs. Beginning in January 1977, ARMCOM will be able to enter probabilities other than those identified by the DODI.
3. In 1975, TARCOM recommended a change to the DoD probabilities based on a study of TARCOM's managed items, TARCOM Report No. 75-35, subject: COSDIF Probabilities for TARCOM. Table 1 presents the probabilities as identified in DODI 4140.42 and those proposed by TARCOM. The proposed probabilities were developed from a study of four years of demand history records on approximately 2,000 TARCOM managed items. TARCOM's probabilities are considerably lower than those arrived at by the DoD and are now being evaluated by TARCOM as to their affect on the number of items stocked, budget, readiness ratio and etc.
4. The approach used in developing ARMCOM's probabilities for replenishment items was to obtain the demand history of ARMCOM managed items. However, the only accessible data was the Nov 76 ALPHA Demand Return Disposal (DRD) file, which contains only 2 years of demand data (from Dec 74 to Dec 76) for the 9,000 ARMCOM managed active items. Since the ALPHA system keeps only the current 2 years of data, a search was made, within the Command, to obtain the oldest Operations Readiness Oriented Supply Status (OROSS) reports. A Jan 76 report was located which summarizes demands over a two year period (Jan 74 through Jan 76) and if merged into the DRD files, will provide a 3 year data base. Since only the DRD files are accessible at this time, the probabilities as developed in this MFR are based on only the two years of demand data.
5. The assumptions and criteria used in developing the replenishment probabilities are as follows:

26 JAN 1971

DRSAR-SAS

SUBJECT: Cost Differential (COSDIF) Probabilities

a. The average yearly demand (demand frequency) of an item is estimated to be the number of demands (requisitions) that occurred in the first of the two years of data, i.e., Dec 74 through Dec 75.

b. The demand probabilities remain constant for the application period, approximately 2 years.

6. The ARMCOM probabilities were developed by determining for each group of items having the same demand frequency, the proportion of the group having no demands in the succeeding year. For example, if 100 items had a demand frequency of 6 in the first year and 40 of those items had no demand in the 2nd year, the proportion would be 0.4. This proportion is an estimate of the probability of having no demands for one year given the demand frequency for the prior year. The square of this proportion is then an estimate of the probability of no demands in two years. Table 2 presents a summary of ARMCOM's 2 years of demand history; the number of those items having a demand frequency of 1 through 12 in the first year; the number of those items having no demand the 2nd year; and, the probability of no demands in the next succeeding years. As shown in Table 2, an item having a demand frequency of 1 has a probability 0.58 of having no demands over a one year period and a probability of 0.34 of having no demands over a two year period. As demand frequency increases the probability of no demands decreases sharply.

7. There are three options available to ARMCOM (Incl 4):

- a. Continue to use the DODI 4140.42 probabilities.
- b. Implement the probabilities developed by TARCOM.
- c. Implement the proposed ARMCOM probabilities.

Table 3 presents each option. There is a significant difference between the DODI set and those listed under TARCOM and ARMCOM, the latter two being considerably lower than DoD's. However, they do not appear to be totally unreasonable, DA Pamphlet 70-5, "Mathematics of Military Action, Operations and Systems", states, "... an item whose average demand rate is one piece per time period will have a probability of nearly 0.4 of showing a history of no demand at all during another time period of the same length." Although the statement refers to quantities, an item that has a demand frequency of 1 per period will have at least an average demand rate of 1 piece per period. A higher piece demand rate would logically lower the probability of no demand; ARMCOM's average number of pieces per demand incidence is 38. The probability of no demand in a two year period for an item having a demand frequency of 1 is 0.44 for TARCOM items and 0.34 for ARMCOM items which compares favorably with the probability of 0.4 as stated in DA Pamphlet 70-5. In comparing the proposed ARMCOM and TARCOM probabilities; ARMCOM's are lower and converge

8 JAN 1971

DRSAR-SAS

SUBJECT: Cost Differential (COSDIF) Probabilities

to zero very sharply (having a value of zero for demand frequencies greater than 7) where TARCOM's probabilities remain relatively constant ranging from 0.04 to 0.11 for demand frequencies of 4 to 12. These differences are caused by various factors, e.g., items peculiar to each Command, degree of item commonality, or total number of items stocked. However, the impact on ARMCOM in either implementing the proposed TARCOM or the proposed ARMCOM probabilities would certainly be an increase in the number of items stocked which in turn, affects ARMCOM's budget, and readiness posture. The degree of the impact and the extent of the impact in dollar savings, to the Army however, is dependent on the accuracy of the probabilities in predicting no demands.

8. In summary, the probabilities prepared by TARCOM and those developed for ARMCOM agree in that both are considerably lower than those identified in the DODI 4140.42. However, ARMCOM's probabilities do differ from TARCOM's; they are generally lower and reach a value of 0.0 for a demand frequency of 8 or more (see Table 3), but these differences may be representative of the differences for each Command's managed items.

9. Recommendations and Conclusions:

a. A study be conducted to determine the dollar impact of implementing the proposed ARMCOM probabilities.

b. The proposed ARMCOM probability set be updated every year for approximately 3 to 5 years and then reviewed every 2 years, thereafter.

James B Beeson

JAMES B. BEESON
Operations Research Analyst
Studies Application Division
Systems Analysis Directorate

4 Incl
as

TABLE 1. COSDIF PROBABILITIES

| <u>DEMAND FREQUENCY*</u> | <u>DODI 4140.42</u> | <u>PROPOSED BY TARCOM</u> |
|------------------------------|---------------------|---------------------------|
| 1 | .82 | .44 |
| 2 | .67 | .32 |
| 3 | .55 | .21 |
| 4 | .45 | .11 |
| 5 | .37 | .10 |
| 6 | .30 | .10 |
| 7 | .25 | .07 |
| 8 | .20 | .08 |
| 9 | .17 | .04 |
| 10 | .14 | .05 |
| 11 | .11 | .04 |
| 12 | .09 | .06 |

*Only those items with demand frequency of 12 or less were considered.

Incl 1

TABLE 2. PROBABILITY OF NO DEMAND BASED ON 2 YEARS OF ARMCOM DATA

| <u>DEMAND FREQUENCY 1ST YEAR</u> | <u>NUMBER OF ITEMS</u> | <u>NUMBER OF ITEMS WITH NO DEMAND IN 2ND YEAR</u> | <u>PROB. OF NO DEMAND IN ONE YEAR</u> | <u>PROB. OF NO DEMAND IN TWO YEARS</u> |
|--|----------------------------|---|---|--|
| 1 | 2,288 | 1,339 | .585 | .34 |
| 2 | 1,039 | 398 | .383 | .15 |
| 3 | 637 | 140 | .22 | .05 |
| 4 | 439 | 85 | .194 | .04 |
| 5 | 343 | 42 | .122 | .01 |
| 6 | 252 | 26 | .103 | .01 |
| 7 | 220 | 23 | .105 | .01 |
| 8 | 169 | 6 | .036 | - |
| 9 | 153 | 8 | .052 | - |
| 10 | 114 | 4 | .035 | - |
| 11 | 111 | 2 | .018 | - |
| 12 | 79 | 4 | .051 | - |

Incl 2

TABLE 3. COSDIF PROBABILITIES FOR REPLENISHMENT TYPE ITEMS

| <u>DEMAND FREQUENCY*</u> | <u>DODI 4140.42</u> | <u>PROPOSED BY TARCOM</u> | <u>PROPOSED ARMCOM SET</u> |
|------------------------------|---------------------|-------------------------------|--------------------------------|
| 1 | .82 | .44 | .34 |
| 2 | .67 | .32 | .15 |
| 3 | .55 | .21 | .05 |
| 4 | .45 | .11 | .04 |
| 5 | .37 | .10 | .02 |
| 6 | .30 | .10 | .01 |
| 7 | .25 | .07 | .01 |
| 8 | .20 | .08 | 0.0 |
| 9 | .17 | .04 | 0.0 |
| 10 | .14 | .05 | 0.0 |
| 11 | .11 | .04 | 0.0 |
| 12 | .09 | .06 | 0.0 |

*Only those items with demand frequency of 12 or less were considered.

Incl 3



DEPARTMENT OF THE ARMY
HEADQUARTERS US ARMY MATERIEL DEVELOPMENT AND READINESS COMMAND
5001 EISENHOWER AVE., ALEXANDRIA, VA. 22313

DRCMM-RS

26 OCT 1976

SUBJECT: Change to Cost Differential (COSDIF) Probabilities

SEE DISTRIBUTION

1. References:

- a. TARCOM Report No. 75-35, subject: COSDIF Probabilities for TARCOM, attached as Inclosure 1.
- b. System Change Request #XSUZZC528701, subject: COSDIF Probabilities, 14 October 1975, attached as Inclosure 2.
- c. AMCSU-KP letter, 5 December 1975, subject: SCR for Conditional Probabilities for Provisioning Items, attached as Inclosure 3.

2. The purpose of this letter is to provide information regarding a potentially significant change to the COSDIF stockage model and provide guidance on the use of this change. At present, one set of COSDIF probabilities is applied to both provisioning items and replenishment type items. This set of probabilities, which is hard-coded in COSDIF, is identified in DODI 4140.42.

3. Beginning in January 1977, CCSS will be able to accommodate two sets of COSDIF probabilities. One set will apply to provisioning items and will remain hard-coded until April 1977 (Release 49). The other set will apply to replenishment type items and can be entered by the NICP following release 47 in January 1977.

4. In applying this added capability, there are several options open to the commodity commands. The NICP may:

- a. Continue to use the set of probabilities cited in DODI 4140.42 for both categories.
- b. Develop their own probabilities.
- c. Elect to use for provisioning items the set developed for the Navy by ALRAND. In no case should this set be used for replenishment items.

Incl 4

DRCMM-RS

SUBJECT: Change to Cost Differential (COSDIF) Probabilities

- d. Elect to use the set developed by TARCOM for replenishment items. In no case should this set be used for provisioning items.
5. In all cases where the command elects to use probabilities other than those identified in the DODI, the command should make an analysis to insure probabilities selected are appropriate and assess budget impact. The Inventory Research Office and ALMSA will provide assistance in this analysis. The command should also be prepared to provide justification for such selections, should the question arise during budget hearings.
6. Any questions regarding this guidance should be discussed with LTC D. Weir, DRCMM-RS, AUTOVON 284-8221.

FOR THE COMMANDER:



3 Incl
as

RONALD N. BOWMAN
Colonel, GS
Assistant for
Secondary Items Programs

DISTRIBUTION:

- ✓ Cdr, US Army Armaments Command, ATTN: DRSTAR-MM-P, Rock Island, IL 61201
- Cdr, US Army Aviation Systems Command, ATTN: DRSAV-QP, St. Louis, MO 63166
- Cdr, US Army Electronics Command, ATTN: DRSEL-MM-P, Ft Monmouth, NJ 07703
- Cdr, US Army Missile Command, ATTN: DRSMI-SOT, Redstone Arsenal, AL 35809
- Cdr, US Army Tank-Automotive Readiness Command, Warren, MI 48090, ATTN: DRSTA-FE
- Cdr, US Army Troop Support Command, ATTN: DRSTA-SX, 4300 Goodfellow Blvd, St. Louis, MO 63101
- Cdr, US DARCOM Automated Logistics Systems Agency, ATTN: DRXAL-MCC, St. Louis, MO 63101
- Ch, DRC Inventory Research Office, Philadelphia, PA 19106

DISTRIBUTION LIST

Copy No.

Commander

US Army Materiel Development and Readiness Command

1 ATTN: DRCMA
1 DRCRD
1 DRCPA-S
5001 Eisenhower Avenue
Alexandria, VA 22333

Commander

US Army Armament Materiel Readiness Command

1 ATTN: DRSAR-CG
1 DRSAR-DCG
1 DRSAR-EN
1 DRSAR-RD
1 DRSAR-CP
27 DRSAR-SA
1 DRSAR-PA
1 DRSAR-PP
1 DRSAR-OP
1 DRSAR-QA
1 DRSAR-IS
1 DRSAR-MM
1 DRSAR-MA
1 DRSAR-AS
1 DRSAR-SF
Rock Island, IL 61201

1 Commander

US Army Test and Evaluation Command

ATTN: DRSTE-SY
Aberdeen Proving Ground, MD 21005

1 Commander

US Army Electronics Command
ATTN: DRSEL-SA
Fort Monmouth, NJ 07703

1 Commander

US Army Missile Command
ATTN: DRSMI-CS
Redstone Arsenal, AL 35809

1 Commander

US Army Tank-Automotive Materiel & Readiness Command
ATTN: DRSTA-S
Warren, MI 48090

DISTRIBUTION LIST (Cont)

Copy No.

- 1 Commander
US Army Tank-Automotive Research & Development Command
ATTN: DRDTA-V
Warren, MI 48090
- 1 Commander
HQ, US Army Aviation Systems Command
ATTN: DRSAV-D
P. O. Box 209, Main Office
St. Louis, MO 64502
- 1 Commander
US Army Troop Support Command
ATTN: DRSTS-G
St. Louis, MO 63120
- 1 Project Manager for Cannon Artillery Weapons Systems
ATTN: DRCPM-CAWS
Dover, NJ 07801
- 1 Commander
US Army Development and Readiness Command
Office of the Project Manager for Selected Ammunition
ATTN: DRCPM-SA
Dover, NJ 07801
- 1 Project Manager for M110E2
ATTN: DRCPM-M110E2
Rock Island, IL 61201
- 1 Project Manager for Air Defense Gun Systems
ATTN: DRCPM-ARGADS
Rock Island, IL 61201
- 1 Product Manager for Production Base Modification & Expansion
ATTN: DRCPM-PBM
Dover, NJ 07801
- 1 Product Manager for Advanced Attack Helicopter Systems
US Army Aviation Systems Command
St. Louis, MO 63166
- 1 Product Manager for AH-1 Cobra Series Aircraft
US Army Development & Readiness Command
P. O. Box 209
St. Louis, MO 63166

DISTRIBUTION LIST (Cont)

Copy No.

- 1 Commander
Rock Island Arsenal
1 ATTN: SARRI-CO
1 SARRI-RL
1 SARRI-ADL
Rock Island, IL 61201
- 1 Commander
Watervliet Arsenal
ATTN: SARVV-CO
Watervliet, NY 12189
- 1 Commander
Picatinny Arsenal
ATTN: SARPA-PA-S
Dover, NJ 07801
- 1 Commander
Edgewood Arsenal
ATTN: SAREA-DE-N
Aberdeen Proving Ground, MD 21010
- 1 Commander
Frankford Arsenal
ATTN: SARFA-PA
Philadelphia, PA 19137
- 1 Commander
Human Engineering Laboratories
ATTN: DRXHE-D
Aberdeen Proving Ground, MD 21005
- 1 Commander
US Army Materiel Systems Analysis Activity
ATTN: DRXSY-D
Aberdeen Proving Ground, MD 21005
- 1 Commandant
US Army Field Artillery Center
Fort Sill, OK 73503
- 1 Commandant
US Army Infantry School
Fort Benning, GA 31905
- 1 Commander
US Army Missile & Munitions Center & School
Redstone Arsenal, AL 35809

DISTRIBUTION LIST (Cont)

Copy No.

- 1 Commandant
US Army Air Defense School
Fort Bliss, TX 79916
- 1 Director
US Army Management Engineering Training Agency
ATTN: DRXON-AMS
Rock Island, IL 61201
- 1 Commander
US Army TRADOC Systems Analysis Activity
White Sands Missile Range
White Sands, NM 88002
- 1 Director
Advanced Research Projects Agency
1400 Wilson Boulevard
Arlington, VA 22209
- 1 Commander
Defense Logistics Studies Information Exchange
Fort Lee, VA 23801
- 1 Commander
US Army Logistics Management Center
ATTN: DRXMC-LS
Fort Lee, VA 23801
- 1 Commander
US Army Logistics Center
ATTN: ATCL-S
Fort Lee, VA 23801
- 12 Defense Documentation Center
Cameron Station
Alexandria, VA 22314